FINAL REPORT

Pre-Concentration for Improved Long-Term Monitoring of Contaminants in Groundwater

SERDP Project ER-1604

JANUARY 2009

Brandy J. White
Paul T. Charles
Brian J. Melde
Naval Research Laboratory

SERDP
DOD ▪ EPA ▪ DOE

Report Documentation Page

Form Approved
OMB No. 0704-0188

1. REPORT DATE	2. REPORT TYPE	3. DATES COVERED
2009	**N/A**	**-**

4. TITLE AND SUBTITLE	5a. CONTRACT NUMBER
Pre-Concentration for Improved Long-Term Monitoring of Contaminants in Groundwater	5b. GRANT NUMBER
	5c. PROGRAM ELEMENT NUMBER
6. AUTHOR(S)	5d. PROJECT NUMBER
	5e. TASK NUMBER
	5f. WORK UNIT NUMBER
7. PERFORMING ORGANIZATION NAME(S) AND ADDRESS(ES) **Naval Research Laboratory**	8. PERFORMING ORGANIZATION REPORT NUMBER
9. SPONSORING/MONITORING AGENCY NAME(S) AND ADDRESS(ES)	10. SPONSOR/MONITOR'S ACRONYM(S)
	11. SPONSOR/MONITOR'S REPORT NUMBER(S)

12. DISTRIBUTION/AVAILABILITY STATEMENT
Approved for public release, distribution unlimited

13. SUPPLEMENTARY NOTES
The original document contains color images.

14. ABSTRACT

Materials for the concentration of nitroenergetic targets from groundwater are sought for monitoring and remediation applications. For this work, periodic mesoporous organosilicas incorporating diethylbenzene bridges in their pore walls were applied for the adsorption of nitroenegetic targets from aqueous solution. The materials were synthesized by co-condensing precursors to improve structural characteristics. Molecular imprinting of the pore surfaces was employed through the use of a novel target-like surfactant to further enhance selectivity for targets of interest (nitroenergetics and their breakdown products) over targets of similar structure (p-cresol and p-nitrophenol). The impact of variations in precursor ratios and amounts of imprint molecule was evaluated. These results were applied to the development of materials possessing organization on both the meso and macro scales. The incorporation of macropores provides a material with enhanced flow through characteristics, thereby reducing back pressure when used in column formats. Concentration of targets from soil sample extracts using these materials was demonstrated.

15. SUBJECT TERMS

16. SECURITY CLASSIFICATION OF:			17. LIMITATION OF ABSTRACT	18. NUMBER OF PAGES	19a. NAME OF RESPONSIBLE PERSON
a. REPORT	b. ABSTRACT	c. THIS PAGE			
unclassified	**unclassified**	**unclassified**	**SAR**	**59**	

Standard Form 298 (Rev. 8-98)
Prescribed by ANSI Std Z39-18

09-1226-0256

PUBLICATION OR PRESENTATION RELEASE REQUEST

NRLINST 5600.2

1. REFERENCES AND ENCLOSURES	2. TYPE OF PUBLICATION OR PRESENTATION		3. ADMINISTRATIVE INFORMATION
Ref: (a) NRL Instruction 5600.2 (b) NRL Instruction 5510.40D Encl: (1) Two copies of subject paper (or abstract)	( ) Abstract only, published ( ) Book ( ) Conference Proceedings (refereed) ( ) Invited speaker ( ) Journal article (refereed) ( ) Oral Presentation, published (✓) Other, explain Published technical report - online	( ) Abstract only, not published ( ) Book Chapter ( ) Conference Proceedings (not refereed) ( ) Multimedia report ( ) Journal article (not refereed) ( ) Oral Presentation, not published	STRN NRL/OT/6900--09-003 Route Sheet No. 6900/003 Job Order No. 69-9629-08 Classification X U Sponsor SERDP approval obtained _____yes _____no

4. AUTHOR

Title of Paper or Presentation

Periodic Mesoporous Organosilicas (PMOs) as Preconcentration Elements for Improved Longterm Monitoring of Key Contaminants in Groundwater

Author(s) Name(s) *(First, Mi, Last)*, Code, Affiliation if not NRL

Brandy J. White (6920), Paul T. Charles (6920)

This is a Final Security Review. Any changes made in the document after approved by Code 1226 nullify the Security Review

It is intended to offer this paper to the _____ *(Name of Conference)*

_____ *(Date, Place and Classification of Conference)*

and/or for publication in SERDP's On-Line Library - http://docs.serdp-estcp.org *(Name and Classification of Publication)* Strategic Environmental Research & Development Program *(Name of Publisher)*

After presentation or publication, pertinent publication/presentation data will be entered in the publications data base, in accordance with reference (a).

It is the opinion of the author that the subject paper (is____) (is not X) classified, in accordance with reference (b).

This paper does not violate any disclosure of trade secrets or suggestions of outside individuals or concerns which have been communicated to the Laboratory in confidence. This paper (does____) (does not X) contain any militarily critical technology.

This subject paper (has____) (has never X) been incorporated in an official NRL Report.

Brandy White; Code 6920 — Name and Code *(Principal Author)*

(Signature)

5. ROUTING/APPROVAL

CODE	SIGNATURE	DATE	COMMENTS
Author(s)			Much of this information has been released previously. Refer to 08-1226-0873; 06-1226-1937; 06-1226-0249; 08-12226-1569; 08-1226-2891; 08-1226-1570.
Brandy White, 6920			
Section Head			
Branch Head			Sponsor's approval attached
Division Head 6900		1/8/09	1. Release of this paper is approved. 2. To the best knowledge of this Division, the subject matter of this paper (has____) (has never X) been classified.
Security, Code 1226		1/26/09	1. Paper or abstract was released. 2. A copy is filed in this office.
Office of Counsel, Code 1008.2		1/30/09	
ADOR/Director NCST 6000 for		03 FEB 2009	
Public Affairs *(Unclassified/ Unlimited Only)*, Code 1030		2/5/09	
Division, Code			
Author, Code			

HQ-NRL 5511/6 (Rev. 12-98) (e)

THIS FORM CANCELS AND SUPERSEDES ALL PREVIOUS VERSIONS

REPORT DOCUMENTATION PAGE

Form Approved
OMB No. 0704-0188

PLEASE DO NOT RETURN YOUR FORM TO THE ABOVE ORGANIZATION.

1. REPORT DATE *(DD-MM-YYYY)*	2. REPORT TYPE	3. DATES COVERED *(From - To)*
12/31/2008	Final Technical Report	01/25/2008

4. TITLE AND SUBTITLE

Periodic Mesoporous Organosilicas (PMOs) as Pre-concentration Elements for Improved Longterm Monitoring of Key Contaminants in Groundwater

5a. CONTRACT NUMBER

MIPR# W74RDV80243004

5b. GRANT NUMBER

5c. PROGRAM ELEMENT NUMBER

6. AUTHOR(S)

White, Brandy J.
Charles, Paul T.
Melde, Brian J.

5d. PROJECT NUMBER

08 ER01-035 / ER-1604

5e. TASK NUMBER

5f. WORK UNIT NUMBER

69-9629-0-8-5

7. PERFORMING ORGANIZATION NAME(S) AND ADDRESS(ES)

Center for Bio/Molecular Science and Engineering
Naval Research Laboratory; Code 6900
Washington, DC 20375

8. PERFORMING ORGANIZATION REPORT NUMBER

9. SPONSORING/MONITORING AGENCY NAME(S) AND ADDRESS(ES)

Department of Defense
Strategic Environmental Research & Development Program
901 N Stuart St., Suite 303
Arlington VA 22203

10. SPONSOR/MONITOR'S ACRONYM(S)

SERDP

11. SPONSOR/MONITOR'S REPORT NUMBER(S)

12. DISTRIBUTION/AVAILABILITY STATEMENT

Approved for public release; distribution is unlimited

13. SUPPLEMENTARY NOTES

N/A

14. ABSTRACT

Materials for the concentration of nitroenergetic targets from groundwater are sought for monitoring and remediation applications. For this work, periodic mesoporous organosilicas incorporating diethylbenzene bridges in their pore walls were applied for the adsorption of nitroenegetic targets from aqueous solution. The materials were synthesized by co-condensing precursors to improve structural characteristics. Molecular imprinting of the pore surfaces was employed through the use of a novel target-like surfactant to further enhance selectivity for targets of interest (nitroenergetics and their breakdown products) over targets of similar structure (p-cresol and p-nitrophenol). The impact of variations in precursor ratios and amounts of imprint molecule was evaluated. These results were applied to the development of materials possessing organization on both the meso and macro scales. The incorporation of macropores provides a material with enhanced flow through characteristics, thereby reducing back pressure when used in column formats. Concentration of targets from soil sample extracts using these materials was demonstrated.

15. SUBJECT TERMS

mesoporous, sorbent, nitroenergetic, extraction

16. SECURITY CLASSIFICATION OF:			17. LIMITATION OF ABSTRACT	18. NUMBER OF PAGES	19a. NAME OF RESPONSIBLE PERSON
a. REPORT	b. ABSTRACT	c. THIS PAGE	UU		Brandy J. White
					19b. TELEPHONE NUMBER *(Include area code)* 202 404 6100

Table of Contents

Table of Contents	i
Acronyms	ii
Figures	v
Tables	vi
Acknowledgements	1
Executive Summary	2
Objective	5
Background	5
- Periodic Mesoporous Organosilicas	6
- PMOs and Electrochemical Detection	10
Materials and Methods	11
- Synthesis of PMOs	11
- Binding Characteristics	13
- HPLC Analysis	13
- Nitrogen sorption/TGA/XRD	13
- Soil and Water Samples	14
- SEM and TEM	15
Results and Accomplishments	15
- Phase I. Materials Development	15
- Phase II. Kinetic and Binding Analysis	33
- Phase III. Contaminant Groundwater Testing	36
Concluding Summary	39
References	43
Appendix A: Supporting Information	45
- Soil Sample Results	45
- Cost Analysis	48
Appendix B: Lists of Technical Publications	49

Acronyms

2,4-DNT	2,4-dinitrotoluene
2-ADNT	2-amino-4,6-dinitrotoluene
2-NT	2-nitrotoluene
3-NT	3-nitrotoluene
4-ADNT	4-amino-2,6-dinitrotoluene
4-NT	4-nitrotoluene
APS	3-aminopropyltrimethoxysilane
BET	Brunauer-Emmett-Teller
BJH	Barrett-Joyner-Halenda
BS	benzene-bridged PMO material
BTE	1,2-bis(trimethoxysilyl)ethane
CMS	corrective measures study
DEB	1,2-bis(trimethoxysilylethyl)benzene
DMB	1,2-bis(trimethoxysilylmethyl)benzene
DNA	2,4-dinitroaniline
DNB	dinitrobenzene
DNB-Brij	Brij 76 modified by esterification with 3,5-dinitrobenzoyl chloride
DOC	dissolved organic carbon
GC	Gas chromatography
HMX	1,3,5,7-tetranitro-1,3,5,7-tetrazocane
HPLC	high performance liquid chromatography
IMS	ion mobility spectrometry
LC	Liquid chromatography
M-0:100	mesoporous material synthesized using 100% BTE
M-0:100 Imp	mesoporous material synthesized using 100% BTE with 12.5% imprint template
M-100:0	mesoporous material synthesized using 100% DEB
M-100:0 Imp	mesoporous material synthesized using 100% DEB with 12.5% imprint template
M-50:50	mesoporous material synthesized using 50% BTE and 50% DEB
M-50:50 Imp	mesoporous material synthesized using 50% BTE with 50% DEB with 12.5% imprint template
M-60:40	mesoporous material synthesized using 60% BTE and 40% DEB
M-60:40 Imp	mesoporous material synthesized using 60% BTE with 40% DEB with 12.5% imprint template
M-70:30	mesoporous material synthesized using 70% BTE and 30% DEB

M-70:30 Imp	mesoporous material synthesized using 70% BTE with 30% DEB with 12.5% imprint template
M-70:30 Imp 100	mesoporous material synthesized using 70% BTE with 30% DEB with 100% imprint template
M-70:30 Imp 25	mesoporous material synthesized using 70% BTE with 30% DEB with 25% imprint template
M-70:30 Imp 50	mesoporous material synthesized using 70% BTE with 30% DEB with 50% imprint template
M-75:25	mesoporous material synthesized using 75% BTE with 25% DEB
M-75:25 Imp	mesoporous material synthesized using 75% BTE with 25% DEB with 12.5% imprint template
M-90:10	mesoporous material synthesized using 90% BTE with 10% DEB
M-90:10 Imp	mesoporous material synthesized using 90% BTE with 10% DEB with 12.5% imprint template
MIP	molecularly imprinted polymer
MM1	heirarchical material synthesized using 50% BET with 50% DEB and 12.6% imprint template
MS	mass spectrometry
NB	nitrobenzene
P10	heirarchical material synthesized using 50% BET, 40% DEB and 10 PTS
P123	Pluronic P123
pCR	p-cresol
PMO	periodic mesoporous organosilica
pNP	p-nitrophenol
PTFE	polytetrafluoroethylene
PTS	phenyltrimethoxysilane
RAM	restricted access materials
RDX	1,3,5-Trinitroperhydro-1,3,5-triazine
REMUS	Remote Environmental Monitoring Units
SEM	scanning electron microscope
SPE	solid phase extraction
SPME	solid phase microextraction
TEM	Transmission electron microscopy
TGA	Thermogravimetric analysis
TMB	mesitylene; 1,3,5-Trimethylbenzene
TNB	trinitrobenzene
TNT	2,4,6-trinitrotoluene
USERDC	US Army Corps of Engineers, Engineer Research and Development Center

UUA	Unmanned Undersea Vehicle
XRD	X-ray diffraction

Figures

Figure 1 Synthesis of periodic mesoporous organosilicas
Figure 2 Siloxane precursors
Figure 3 Adsorption of analytes by original imprinted PMO
Figure 4 Breakthrough curves for original PMOs
Figure 5 Comparison of imprinted and non-imprinted PMOs
Figure 6 Competitive binding of TNT and RDX
Figure 7 Electrochemical detection of TNT
Figure 8 Concentration dependence for electrochemical detection
Figure 9 Synthesis of imprint template
Figure 10 Photos of soil sample collection sites
Figure 11 Impact of bridging group variations
Figure 12 Bridging group variations in imprinted and non-imprinted materials
Figure 13 XRD spectra for mesoporous materials
Figure 14 Pore diameter distributions for mesoporous materials
Figure 15 Nitrogen sorption isotherms for mesoporous materials
Figure 16 TNT binding isotherms for imprinted mesoporous materials
Figure 17 Double reciprocal plots for imprinted mesoporous materials
Figure 18 SEM and TEM images of MM1
Figure 19 XRD spectra for heirarchical materials
Figure 20 Pore diameter distributions for hierarchical materials
Figure 21 Nitrogen sorption isotherms for hierarchical materials
Figure 22 Homogeneity plots for heirarchical BTE:DEB materials
Figure 23 TNT binding isotherm for MM1
Figure 24 SEM and TEM images of P10
Figure 25 RDX binding isotherm for P10
Figure 26 TNT binding kinetics for MM1
Figure 27 RDX bidinding kinetics for P10
Figure 28 Homogeneity plot for MM1
Figure 29 Homogeneity plot for P10
Figure 30 MM1 v. Activated charcoal column
Figure 31 P10 v. Activated charcoal column
Figure 32 Binding of targets from complex matrices
Figure 33 Temperature and pH dependence
Figure 34 Comparison of MM1 to commerical resins
Figure 35 Concentration of soil extract HO-001
Figure 36 Concentration of soil extract HO-022
Figure 37 Summary of soil extract experiments
Figure 38 Alternative imprint template for paraoxon
Figure 39 Images of SubChem projects

Tables

Table 1	Co-condensate materials characteristics and binding capacities
Table 2	Imprint variant materials characteristics and binding capacities
Table 3	Targets bound from multi-target samples
Table 4	Fit parameters and calculated constants from TNT binding isotherms
Table 5	Targets bound from mixed samples
Table 6	Heterogeneity as indicated by ratios of target adsorption from single and multi-target solutions
Table 7	Structural characteristics for varying DEB to BTE ratios in the hierarchical materials
Table 8	Structural characteristics for varying nitric acid concentrations in the hierarchical materials
Table 9	Structural characteristics for varying mesitylene concentrations in the hierarchical materials
Table 10	Fit parameters and calculated constants for MM1 and P10 materials
Table 11	Soil samples

Acknowledgements

The research described in this final report was supported by the U.S. Department of Defense, through the Strategic Environmental Research and Development Program (SERDP) and through the Office of Naval Research via Naval Research Laboratory funding (Work Unit #69-8764). Dr. Andrea Leeson, Sarah Hunt, Deanne Rider, and other SERDP staff are gratefully acknowledged for their assistance and support.

Dr. Brian Melde's (Nova Research, Inc.) efforts on this project were invaluable. He was responsible for synthesis of the sorbents as well as characterization by TGA, XRD, and nitrogen sorption. Mr. Michael Dinderman (Naval Research Laboratory) provided TEM and SEM support for the project.

Soil samples were provided to us by Alan Hewitt of the US Army Corps of Engineers, Engineer Research and Development Center. Kim Granzow and Michael Dale from the New Mexico Environment Department, Department of Energy Oversight Bureau provided groundwater samples.

Executive Summary

In the U.S. there exist a number of sites that are contaminated with one or more compounds related to weapons technologies. Key contaminants include energetic compounds such as TNT, RDX, and HMX; chlorinated hydrocarbons such as tetrachloroethene and trichloroethene; and degradation products of these contaminants. These compounds pose a threat to the environment and to personnel exposed to the compounds. Long-term monitoring of sites undergoing remediation as well as sites which may eventually require cleanup is critical. Several portable technologies exist which can be applied to the monitoring of key contaminants. The difficulty arises when detection of trace levels in complex matrices is necessary. A number of methods have been explored for concentration of target analytes from groundwater and other real-world samples. Major drawbacks have included the enormous amount of solvent used in extraction processes, time-consuming steps, and necessary conditioning processes. The work described here is directed at the development and evaluation of periodic mesoporous organosilica (PMOs) materials for the pre-concentration of trace level explosives. These materials have the potential to provide improved sensor performance through semi-selective concentration of targets prior to analysis.

Periodic mesoporous organosilicas (PMOs) are organic-inorganic materials with highly ordered pore networks and large internal surface areas (typically >1,000 m^2/g). The structure of the materials is directed by surfactant micelles. Removal of the surfactant following condensation of the siloxane precursors results in a porous structure with a number of possible configurations. These materials can be synthesized with narrow pore size distributions and few blocked pores or obstructions facilitating molecular diffusion throughout the pore networks. The alternating siloxane and organic moieties give PMOs properties associated with both organic and inorganic materials. The siloxane groups provide the structural rigidity required to employ a template method while allowing for incorporation of a unique method for engineering porosity. If one were to prepare a composite with a conventional organic polymer using surfactant templates, the removal of the surfactant templates would result in structural collapse of the polymer due to its flexibility on the molecular scale. In addition to structural rigidity, the silica component of the PMOs provides a degree of hydrophilic character useful for applications in aqueous systems. Organic functional groups within the PMO matrix offer those interactions with targets typically associated with organic polymers. Precursors containing different organic bridging groups have been used to produce a variety of PMOs with unique chemical properties. Experimental parameters, such as the selection of different precursors, surfactants, and functional silanes, allow the design of porous materials with structural and chemical properties optimized for a given application.

Prior to the beginning of this effort, we had demonstrated that PMOs could be engineered to provide semi-selective sorbents for nitroenergetic compounds. The kinetics of these early materials were rapid with equilibrium approached in less than 3 min. These materials had several shortfalls including limited selectivity and high back pressure when applied in column format. The one year program described in this report focused on overcoming these limitations and demonstrating the potential of the optimized sorbents for concentration of targets from real-world samples to provide enhanced detection using existent sensor systems.

Optimization of the sorbents progressed from the early materials mentioned above. During the development of those sorbents, it became apparent that sorbents with diethylbenzene bridging groups offered the highest affinities for nitroenergetic targets. The large organic structure of this group, unfortunately, disrupts the structure of the sorbents resulting in small pores (<20 Å), reduced surface area, and a high degree of disorder in the materials. We used a co-condensation approach to mediate these issues. Through the use of a mixture of 1,4-bis(trimethoxysilylethyl)benzene (DEB, 30%) with 1,2-bis(methoxysilyl)ethane (BTE, 70%), we were able to balance the desirable binding and structural characteristics. In addition, a new imprint template was developed. Previous materials had employed decylamine dinitrobenzene as a target analog. This compound was mixed with the surfactant with the intention that the dinitrobenzene head group would be in contact with the pore walls during condensation. This approach yielded only marginal success. Through modification of the surfactant (Brij®76) using a target analog (3,5-dinitrobenzoyl chloride), we were able to significantly improve the results of imprinting these materials. Enhancement in selectivity and capacity were obtained.

Back pressure issues were address by altering the synthesis protocol to include a larger surfactant (Pluronic P123) and a swelling agent (mesitylene). These changes allowed for incorporation of more DEB (50%) while avoiding the adverse impact on structural characteristics. In addition, these materials have order on two length scales. First, the mesopore structure of the materials described above is maintained. The materials are ordered as indicated by both TEM and XRD, and the pore sizes are larger (~50 Å compared to ~30 Å) than those of the Brij®76 materials. Second, large pores (~1 μm) increase the interconnectivity between the mesopores of the materials and reduce the resistance to sample flow through. The imprinting technique described above (now using modified Pluronic P123) is effective at enhancing the selectivity of these materials. The hierarchical materials can be applied in column formats using gravity or peristaltic pumps to drive fluid flow. Batch experiments indicated that the materials perform over a range of temperatures (4 to 40°C) and will extract targets from sea water, solutions of varying pH (4.5 to 9.0), groundwater, and soil sample extracts.

Pre-concentration of targets from deionized water was demonstrated. In these studies, the hierarchical sorbents yielded eluate concentrations slightly higher than those of two commercial resins described for the concentration of nitroenergetics. Elution of targets from the sorbent was demonstrated using either methanol or acetonitrile. A series of soil sample extracts was prepared from samples collected at Holloman Air Force Base, Alamogordo, NM. The soil samples were extracted using water only which was subsequently filtered and applied to the column (10 mL). Elution from the column was accomplished using methanol (1 mL). Enhancement in the concentration of a number of compounds was achieved. Some of the targets analyzed were RDX, TNB, DNB, TNT, 2,4-DNT, 2- and 4-ADNT. A single column was used for the concentration of more than 75 samples including soil extracts, groundwater, and laboratory preparations with no loss in function.

We have also been able to show that the imprinting technique developed during the course of this program is adaptable to the generation of templates against other targets of interest. We have imprinted a porous material using Pluronic P123 modified using diethyl chlorophosphate, an analog for paraoxon. In addition to pesticide selective sorbents, we have developed materials for the adsorption of phosgene and solvents including benzene and hexane. Interest in these types of materials for the concentration of compounds such as trichloroethylene and tetrachloroethylene has been expressed, and a company is interested in evaluating the potential of these materials for use with gas chromatography systems. A group working to design an

electrochemical sensor for use with Remote Environmental Monitoring Units (REMUS) is planning to use the materials developed during the course of this program to pre-concentrate nitroenergetic targets from sea water. In addition to these types of active monitoring applications, the material developed during the course of this program has the potential for deployment for short- and long-term passive monitoring similar to the polyethylene passive sampling materials.

Objective

This work sought to develop and demonstrate the potential of porous nanostructures as a cost effective, regenerable mechanism for the pre-concentration and long-term monitoring of energetic materials contained in groundwater plumes from testing and training facilities. If successful, integration of the proposed materials into existing field deployable systems would enhance the sensitivity of those systems by orders of magnitude. The goal here was to complete the development of methods for the synthesis of periodic mesoporous organosilicas (PMOs) in order to provide semi-selective sorbents for the pre-concentration of key contaminants in groundwater. At the onset of this program, preliminary work toward establishing these methods had been completed, but only a minimum demonstration of the materials function had been achieved. This work was intended to demonstrate the potential of the materials in bench-top experiments using laboratory generated and real-world samples. Specifically, materials and methods were sought which would provide enhancement of the sensitivity of currently available sensor systems (i.e., IMS, GC/MS, electrochemical) through concentration of trace amounts of environmental pollutants from large sample volumes. These studies focused on designing sorbents for the concentration of nitroenergetics and their degradation products.

Background

In the U.S. there exist over 12,000 sites that are contaminated with one or more compounds related to weapons technologies. These sites are former and current testing and training facilities where waste from weapons manufacture, storage, and reclamation processes has leached into the soil and groundwater.[1] Key contaminants include energetic compounds such as TNT, RDX, and HMX; chlorinated hydrocarbons such as tetrachloroethene and trichloroethene; and degradation products of these contaminants. These compounds pose a threat to the environment and many are known carcinogens or suspected cancer causing agents.[2; 3] One issue has been the potential health hazard posed to military personnel and their families resident on these installations, but the migration and leaching of these carcinogens to the surrounding population, agricultural regions, and neighboring wildlife is also a serious concern.[4; 5] Long-term monitoring of sites undergoing remediation as well as sites which may eventually require cleanup is critical.

Several portable technologies exist which can be applied to the monitoring of key contaminants. The difficulty arises when detection of trace levels in complex matrices is necessary. A number of methods have been explored for concentration of target analytes from groundwater and other real-world samples: liquid-liquid extraction, salting-out techniques, and solid-phase extraction (SPE).[6; 7] Major drawbacks have included the enormous amount of solvent used in extraction processes, time-consuming steps, and necessary conditioning processes. Solid-phase microextraction (SPME) fibers provide a method of pre-concentrating contaminants prior to analysis by high performance liquid chromatography (HPLC), ion mobility spectrometry (IMS), or gas-chromatography mass spectrometry (GC-MS) [8] and yield detection levels typically in the low nanogram per milliliter (ng/ml) range. Unfortunately, SPME fibers require long incubation times and degrade over repeated use. Restricted access materials (RAM) are porous graphite or bifunctional sorbents that have been combined with liquid chromatography-mass spectrometry (LC-MS) to provide enhanced sensitivity (low pg/ml).[9] However, the increased pressure and biofouling associated with the RAM has resulted in higher

variability in sample analysis. Resins packed as columns also have demonstrated some promise for the preconcentration of trace contaminant levels resulting in enhanced HPLC sensitivities of up to three orders of magnitude.[10] The work described here is directed at the development and evaluation of periodic mesoporous organosilica (PMOs) materials for the pre-concentration of trace level explosives. These materials have the potential to provide improved sensor performance through semi-selective concentration of targets prior to analysis.

Periodic Mesoporous Organosilicas (PMOs)

Periodic mesoporous organosilicas (PMOs) are organic-inorganic polymers with highly ordered pore networks and large internal surface areas (typically >1,000 m^2/g). First reported in 1999 [11-13], PMOs are synthesized using a surfactant template approach [14-16] and have narrow pore size distributions with few blocked pores or obstructions facilitating molecular diffusion throughout the pore networks. The alternating siloxane and organic moieties give PMOs properties associated with both organic and inorganic materials.[17; 18] The siloxane groups provide the structural rigidity required to employ a template method while allowing for incorporation of a unique method for engineering porosity. If one were to prepare a composite with a conventional organic polymer using surfactant templates, the removal of the surfactant templates would result in structural collapse of the polymer due to its flexibility on the molecular scale. In addition to structural rigidity, the silica component of the PMOs provides a degree of hydrophilic character useful for applications in aqueous systems. Organic functional groups within the PMO matrix offer those interactions with targets typically associated with organic polymers. Precursors containing different organic bridging groups have been used to produce a variety of PMOs with unique chemical properties. Experimental parameters, such as the selection of different precursors, surfactants, and functional silanes, allow the design of porous materials with structural and chemical properties optimized for a given application.

Figure 1 shows a typical protocol for the synthesis of one of the PMO materials. The surfactant and imprinting template (also a surfactant) are mixed in acidified ethanol at concentrations exceeding the critical micelle concentration. Various packing conformation for the micelles are possible depending on the choice of surfactant, acid, temperature, and concentration. When the micelles are established, the siloxane precursors are added in a drop wise manner to the solution. Condensation of the precursors results in a structure in which regions of surfactant and silicate alternate. Extraction of the surfactant, typically through refluxing, results in a porous structure. The organization of the pores is a result of the organization of the original micelles.

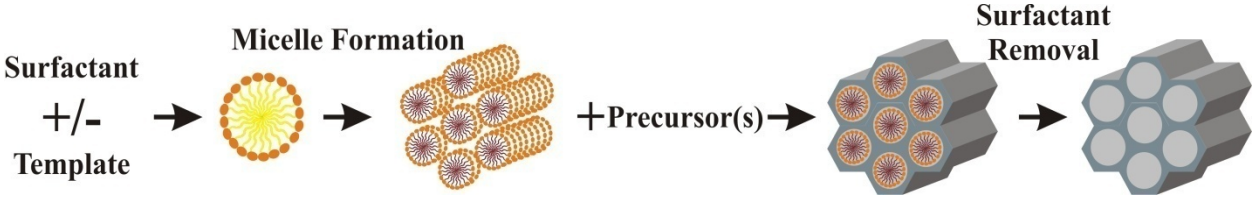

Figure 1. *Synthesis of periodic mesoporous organosilicas (PMOs).*

The tunable nature of these materials results from the potential for selecting various surfactants, imprint templates, and precursors. Figure 2 shows some of the precursors that have been applied by this group to the synthesis of these materials. 1,4-bis(trimethoxysilylmethyl)benzene (DMB) provides affinity for TNT, but materials synthesized

with 1,4-bis(trimethoxysilylethyl)benzene (DEB) were found to provide higher affinity. Materials synthesized using 1,4-bis(trimethoxysilyl)benzene tend to be more organized (increased pore organization and surface area) than those synthesized using DEB and provide a strongly hydrophobic surface that is useful for the adsorption of solvents like hexane.[19] 3-Aminopropyl)trimethoxysilane (APS) provides primary amine groups which facilitate post synthesis modification. These groups have been used to provide sites at which catalysts can be attached. Further options can be obtained through combining two or more precursors in a co-condensation approach. For example, high binding capacities for phosgene have been obtained through co-condensation of APS and 1,2-bis(trimethoxysilyl)ethane. The material can be modified post-synthesis with a copper metalloporphyrin resulting in a highly porous, well organized material (surface area 1002 m^2/g; pore volume 1.19 cm^3/g; pore diameter 77 Å) with a high concentration of functional sites (unpublished results; [19]).

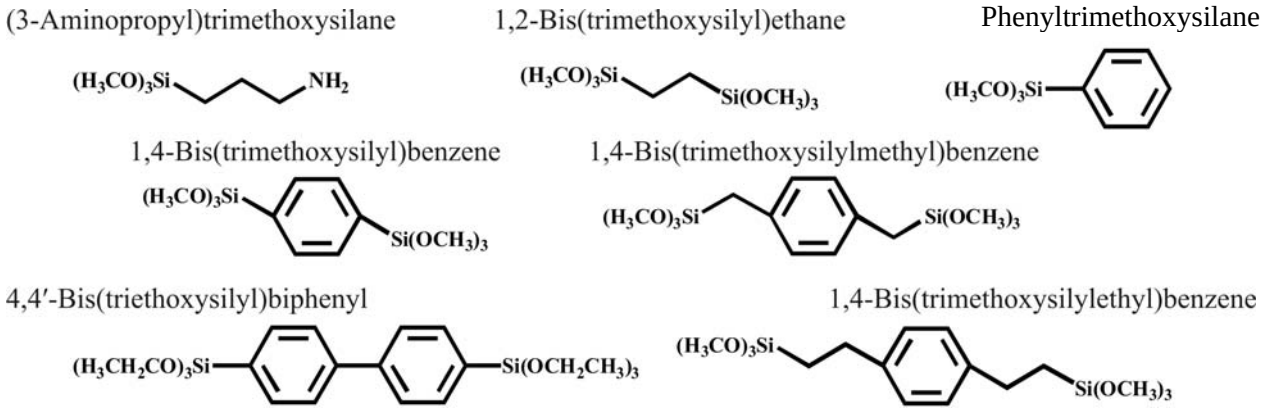

Figure 2. *Siloxane precursors.*

The organization of the PMO materials is directed by the surfactant micelles though it can be disrupted by poor choices of precursors and/or precursor concentrations. The surfactant most commonly employed in the syntheses outlined in Figure 1 is Brij®76 (polyoxyethylene (10) stearyl ether, $C_{18}H_{37}(OCH_2CH_2)_nOH$, n~10). This is an alkylene oxide surfactant. In general, pore sizes of about 30 Å are possible using Brij®76 under these conditions. Various pore organizations are possible including hexagonal, cubic, lamellar, and worm-like. Pore organization is dependent on the conditions of the synthesis including temperature and acid concentration. Variations in the concentrations of hydrophobic compounds, such as hydrophobic precursors, may alter the micelle conformation and, therefore the pore organization.

The surface of the pore results from the interactions between the head groups of the micelles and the siloxane precursors during condensation. The primary mechanism for adsorption of aromatic compounds by the PMO material is the π-π interactions existing between an aromatic target and the bridging groups of the PMO. We have found it possible to enhance the favorable interactions between these materials and targets of interest through "imprinting" the surface of the pores against a target analog. This target-like surfactant becomes part of the surfactant micelles around which the precursor materials form the porous structures of the PMO materials. The idea is similar to that used with molecularly imprinted polymers (MIPs). In the case of MIPS, polymerization is accomplished in the presence of a target (or target analog) which is then extracted from the pore. This process leaves a cavity that is structurally and electronically

complimentary to the target in the material. The result with the PMOs is not quite as exact, but we have demonstrated that the surface interactions with targets are enhanced. This process provides enhanced selectivity in complex mixtures as well as enhanced capacity and affinity in some cases. The specificity obtained through careful selection of precursors as well as imprinting of the PMO surfaces gives the PMOs an advantage over options such as C8, C18, or other silicas. Silica phases function primarily through simple hydrophobic interactions and to some extent size exclusion.

Prior to the beginning of this program, we had demonstrated that, in batch studies, an arylene-bridged PMO preferentially adsorbed aromatic hydrocarbons.[20] Greater than 96% of p-nitrophenol, p-chlorophenol, and p-cresol were absorbed from aqueous solutions within the first minute of PMO contact with greater than 99% adsorbed within 15 minutes. Further studies using a DEB-bridged PMO demonstrated that a degree of selectivity could be achieved for TNT over structurally similar compounds. In a competitive adsorption environment containing p-nitrophenol, p-cresol, and TNT, greater than 85% of TNT adsorption was completed within the first minute of contact (Figure 3).

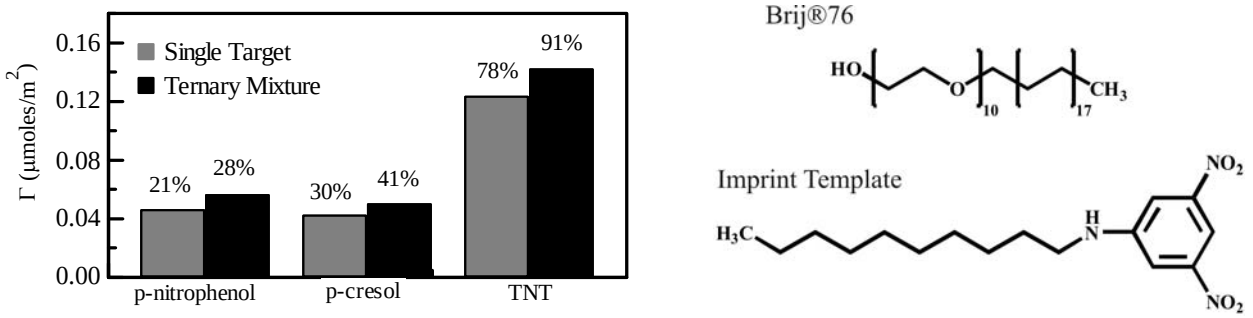

Figure 3. *Adsorption of analytes by a molecularly-imprinted PMO from single target and ternary target solutions. Γ is the amount of target bound per unit surface area. Percentages are of the total target concentration in the sample. Also shown are the structure of Brij®76 and the imprint template molecule used.*

The target binding capacity of the arylene-bridged PMO material was compared to that of activated carbon by monitoring target breakthrough using 1 mM p-nitrophenol. No breakthrough (the entire target in the applied solution was bound) was observed for the first 20 applied bed volumes (Figure 4a). The same weight of activated carbon adsorbed 60 applied bed volumes before breakthrough was observed. While this indicates a PMO target capacity somewhat lower than that of commercially available activated carbon, the activated carbon materials cannot be applied to pre-concentration since targets cannot be easily eluted from them. In the case of the organosilica materials, desorption of the p-nitrophenol can be accomplished by a simple alcohol wash. After 10 adsorption-desorption cycles, no loss of adsorption capacity or performance was observed (Figure 4b). Similar treatment of the activated carbon failed to remove any detectable amount of nitrophenol.

Figure 5a and 5b illustrate the increase in TNT adsorption for the PMO materials upon imprinting with a target analog. Binding of p-nitrophenol almost doubled from 47 nmoles/m^2 to 89 nmoles/m^2 while TNT binding increased from 128 nmoles/m^2 to 155 nmoles/m^2 in single target samples (similar increases are also shown in multiple target samples as illustrated). Equally important is the fact that little increase was observed for p-cresol. In fact, an increase of less than 10% was seen emphasizing the preferential binding of nitro-substituted compounds by the imprinted PMO. As illustrated in Figure 5b, the imprinted material also preferentially binds

TNT from multi-target mixtures where TNT binding was nearly double that of the other compounds present. Figure 6 illustrates the adsorption of TNT and RDX from soil extract. Soil extracts were obtained by mixing 2 g of soil collected at Umatilla Army Depot Activity (Umatilla, OR) with 10 mL acetone. Particles were allowed to settle for 15 min before the supernatant was filtered using a 0.22 μm syringe filter. In this case, the binding of TNT was increased by more than 7-fold as a result of the imprinting process. Although this PMO was originally targeted for TNT, a 4-fold increase in RDX binding was also realized. This further indicates preferential binding of nitro-moieties in the target mixture by the PMO even in the presence of a high dissolved organic carbon (DOC) concentration.

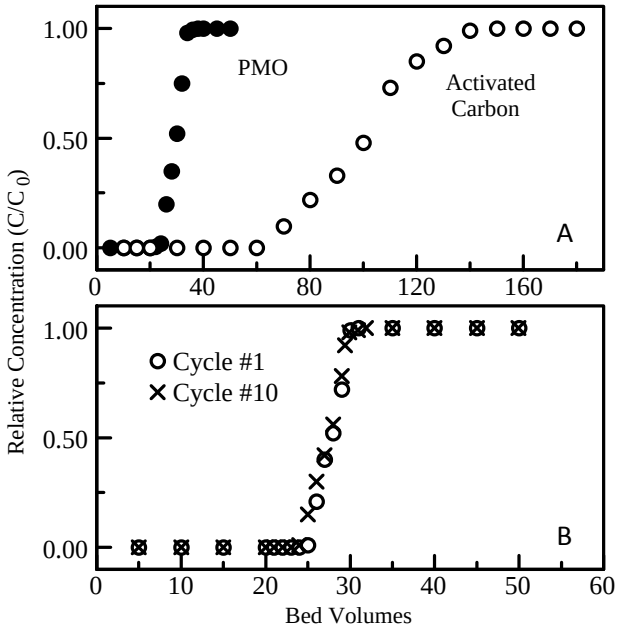

Figure 4. **A.** *Break through curves comparing the PMO to activated carbon are presented as the ratio of the eluent concentration to the initial sample concentration.* **B.** *Effect of ethanol washes on PMO adsorption performance over 10 cycles is presented as a ratio of the target concentration in the eluent versus that of the initial sample.*

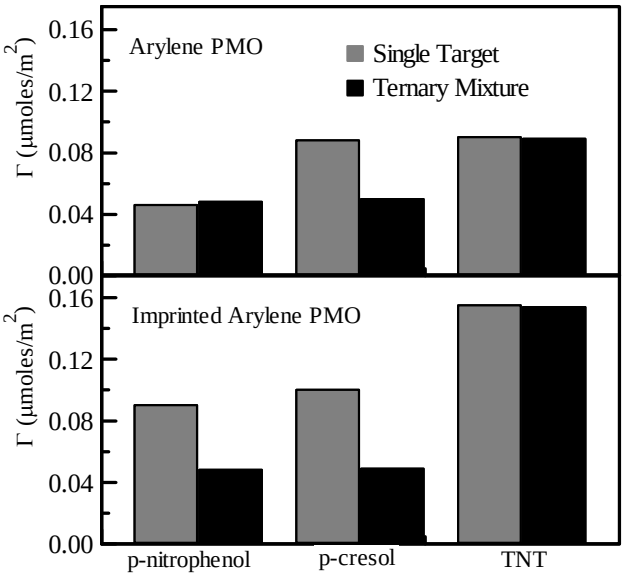

Figure 5. *Adsorption study using non-imprinted (a) and imprinted (b) arylene-bridged PMO from single target and ternary target solutions. Γ is the amount of target bound per unit surface area.*

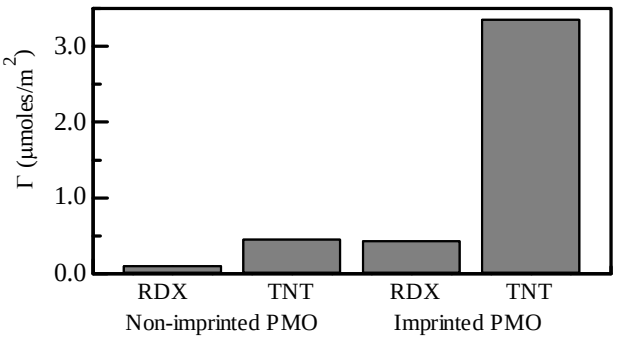

Figure 6. *Competitive binding of TNT and RDX from contaminated soil extract by arylene-PMO.*

PMOs and Electrochemical Detection

Preliminary studies have been conducted using PMO materials for the rapid pre-concentration and extraction of TNT for enhancement of electrochemical analysis. Electrochemical methods have shown promise for the detection of TNT.[21; 22] The PMOs used as pre-concentration materials were imprinted against TNT and employed a benzene (BS) hybrid organic-inorganic polymer. Samples ranging from 0.5 mL to 10 mL containing 5 to 1000 ppb TNT in phosphate buffer were concentrated in-line before electrochemical detection using a micro-column containing 10 mg of the PMO. TNT was rapidly eluted from the column using 40% acetonitrile in 10 mM PBS. Square wave voltammetry was used to monitor the reduction of TNT in an electrochemical flow cell using a carbon working electrode and an Ag/AgCl reference electrode (Figure 7). Using the benzene-bridged PMO material, TNT detection levels of 10 ng/ml (ppb) were obtained when TNT was concentrated from a 2 mL original sample volume (Figure 8). It was also noted that nearly 100% recovery of TNT from the columns was achieved. This can be observed by noting that the areas under the peaks in Figure 7 are identical in all three cases. The benzene-bridged PMO provided the greatest enhancement in sensitivity owing to the rapid elution of TNT from that material as compared to the diethylbenzene-bridged material.

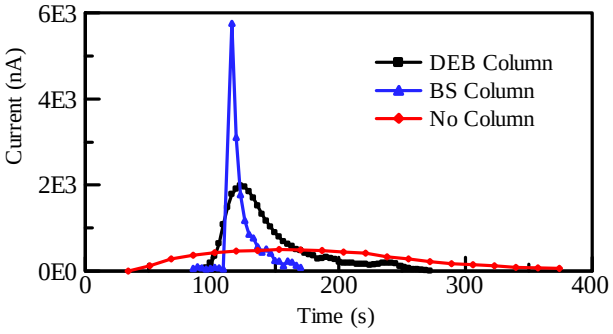

Figure 7. *Electrochemical detection of TNT at 1000 ppb using square-wave voltammetry (SWV) by means of an electrochemical flow cell with a glassy carbon electrode and an Ag/AgCl reference. SWV parameters: Potential range, 0.3 to - 0.8 V vs. Ag/AgCl at a frequency of 100 Hz and an amplitude of 25 mV. Flow rate 200 μL/min. Data obtained using 0.5 mL original sample volumes.*

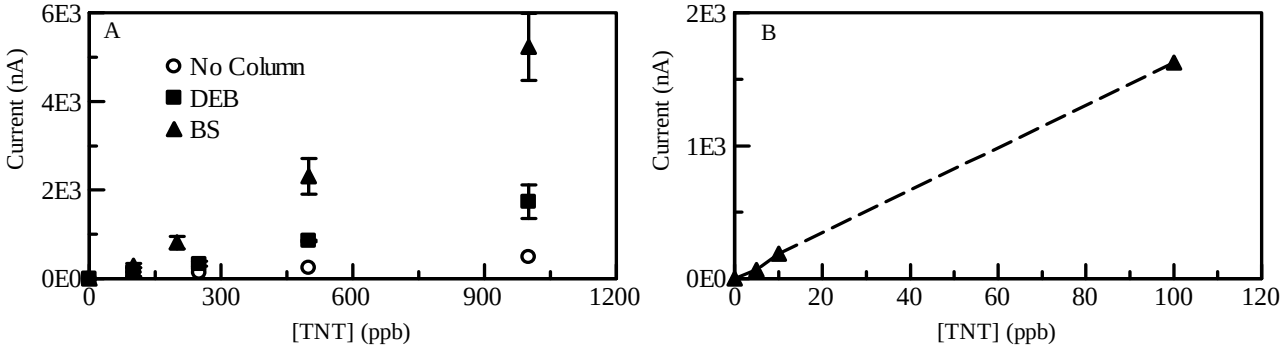

Figure 8. *Peak current versus TNT concentration for the electrochemical detection of TNT using square-wave voltammetry. Presented data compares results obtained without pre-concentration to results obtained using benzene-bridged PMO and diethylbenzene-bridged PMO materials in-line with the detector.* **A.** *0.5 mL original sample eluted in 0.5 mL from BS and DEB column.* **B.** *2 mL original sample eluted in 0.5 mL from BS column.*

Materials and Methods

This program was approached in three stages: Phase I- Material Synthesis, Characterization, and Optimization; Phase II - Kinetics and Binding Analysis; and Phase III- Bench /Pilot Scale Demonstration. Beginning with lessons learned from the studies reported above (Background section), materials were optimized to provide balance between structural and binding characteristics in order to provide stand-alone or in-line concentration of targets. Upon successful synthesis of material with the necessary characteristics, batch studies were conducted to characterize the binding affinities, capacities and kinetics. Finally, column formats were used to evaluate the adsorption and elution characteristics under varying conditions including the use of soil extracts and ground water samples.

Synthesis of PMOs.

Mesoporous Materials.

The first step toward producing materials for these applications was synthesis of a new type of imprinting template. The template used previously (Figure 3) provided marginal results at best and could only be used in low concentrations in the surfactant mixture. To alleviate these issues, we employed esterification of the surfactant head groups to provide a template that would fully integrate with the surfactant. This allows incorporation of a higher concentration of the template as well as providing enhanced contact between the target analog and the pore surfaces during condensation. Figure 9 illustrates the synthesis of the new imprint template.

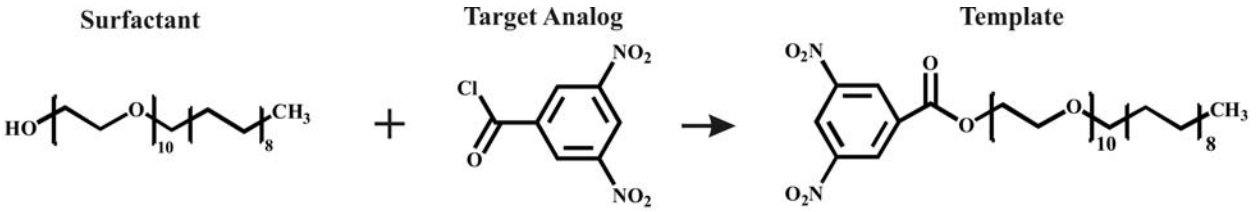

Figure 9. *Synthesis of imprint template for use with Brij®76 surfactant micelles.*

Synthesis of the template was adapted from a protocol used to separate aliphatic alcohol ethoxylates.[23] Briefly, Brij®76 (2g; 2.81 mmol) and 3,5-dinitrobenzoyl chloride (1.3 g; 6 mmol) were dissolved in 60 mL of dichloromethane. Magnesium turnings were added and the mixture was refluxed for 2 h. The liquid was shaken with 60 mL 2% $NaHCO_3$ in a separatory funnel. The organic phase was then extracted and evaporated under vacuum. The resulting dinitrobenzne (DNB)-modified Brij®76 was orange in color.

In order to achieve the goals of this program, we decided to use a co-condensation approach combining DEB and 1,2-bis(methoxysilyl)ethane (BTE; Figure 2). DEB (as described above) had previously been demonstrated to provide binding affinity for TNT. This was a new approach for our group which we hoped would provide a compromise between materials characteristics and binding characteristics. The materials reported in the Background section had little order and poor interconnectivity between the pores. The result was an inability to access all of the surface area of the materials. We hoped to improve these characteristics which would effectively increase the number of binding sites per gram of material as well as the diffusion of target throughout the materials. In addition, the use of a new imprint template necessitated determining the optimum concentration of that compound to be incorporated into the surfactant mixture.

Tables 1 and 2 provide the naming schemes for the various PMO materials. A material synthesized using 70% BTE and 30% DEB with no imprint is referred to as M-70:30. The 70% BTE 30% DEB materials synthesized using 12.5% or 25% modified Brij surfactant are referred to as M-70:30 Imp and M-70:30 Imp 25, respectively.

Our preparation method for the PMOs using Brij®76 surfactant in acidic media has been described previously.[24; 25] Aqueous HCl reaction solution was prepared by adding 13.1 mL concentrated HCl to 186.9 mL of H_2O. Brij®76 (4.0 g) or a combination of Brij®76 and imprint surfactant was dissolved in the HCl solution with stirring at 50 ºC in a closed container. Organosilane (0.0281 mol) (BTE, DEB, or a combination of) was added drop wise to the stirring mixture. Stirring was continued at 50ºC for at least 12 h as a white precipitate formed. The stirring was stopped and the mixture was heated at 70ºC for 24 h. Product was collected by vacuum filtration. Surfactant was extracted by refluxing the product in 1 M HCl in ethanol three times for at least 12 h. The powder was rinsed with copious amounts of ethanol and water and dried under vacuum at 80ºC. Thermogravimetric analysis did not measure any mass loss due to residual surfactant in samples after extraction.

Hierarchical Materials.

Previous work had indicated the potential for back pressure issues when PMOs were employed in column formats. Often, PMOs are mixed with sand to reduce the pressure needed to drive solutions through the columns. This decreases the binding sites within the column. In addition, the PMOs often compact over time resulting in increased back pressure. In order to address these issues, we evaluated the potential of hierarchical silicate materials. These materials were synthesized using a procedure very similar to that of the PMOs. Pluronic P123 is employed as the surfactant, and a swelling agent (mesitylene) was used. The resulting materials have order on two length scales: mesopores (~40 to 80 Å) are within macropores (~1 μm). The large pores provide a much more open pore network facilitating flow through the materials as well as access to the smaller pores. The materials can be imprinted in the same manner as the PMOs, and the same precursors can be used. Optimization of these materials involved determining the proper ratios of precursors (using PMO experiments as a guide), optimum concentration of imprint template, acid concentration, and mesitylene concentration.

In order to prepare imprint template for these materials, esterification of Pluronic P123 with 3,5-dinitrobenzoyl chloride was accomplished as follows: 8 g P123, 1.27 g 3,5-dinitrobenzoyl chloride, and Mg turnings were added to 60 mL dichloromethane and refluxed for 2 h. The solution was shaken with 60 mL 2% aqueous $NaHCO_3$. The organic phase was collected and evaporated to yield the yellow derivatized surfactant.

Synthesis of the hierarchical materials was accomplished as follows: 1.9 g Pluronic P123 was dissolved with mesitylene (TMB, concentration as indicated) in 0.1 M HNO_3 (amount as indicated) with stirring at 60 ºC. For imprinted materials, 1.66 g P123 was combined with 0.24 g 3,5-dinitrobenzoyl modified P123. The stirring solution was allowed to cool to room temperature, and a siloxane mixture consisting of 7.84 mmol total bis-silane (BTE + DEB) was added drop wise. The reaction mixture was stirred until homogeneous, and transferred to a culture tube which was sealed tightly and heated at 60 ºC over night (approximately 18 h). A white gel formed during this period. The tube was unsealed and heated at 60 ºC for 2 days followed by incubation at 80 ºC for an additional 2 days. The product, in the form of a white monolith, was refluxed three times in ethanol for at least 12 h to extract P123, a process that broke the monolith and produced a powder. The powder was collected by suction filtration,

rinsed with ethanol and water, and dried at 100 ºC. Thermogravimetric analysis showed that a small amount of P123 remained in a final product.

Binding Characteristics.

Two types of experiments were used to characterize the binding capacity and affinity of the materials synthesized. Batch experiments were used in all cases where it was necessary to down select from a large number of possible materials (i.e., materials with various ratios of precursors) and for determining saturation capacities and binding affinities. Column studies were used to provide thorough characterization of those materials deemed the most likely candidates through batch studies.

Batch experiments were conducted in 20 mL scintillation vials (EPA Level 3; clear borosilicate glass; PTFE/silicone-lined cap). A fixed mass of PMO or hierarchical material (commonly 15 mg) was weighed directly in the vial using an analytical balance. Target samples were prepared in 18 MΩ Milli-Q deionized water unless otherwise indicated. Sample volumes were 20 mL unless otherwise indicated. Target solutions were added to the sorbents in the vials, and a portion of the sample was retained for use as a control during HPLC analysis. A series dilution of the retained sample was prepared for generation of a standard curve allowing for analysis of target binding by the sorbents. The vials were incubated overnight (unless otherwise indicated) on rotisserie mixers. Following incubation, samples were filtered using 25 mm Acrodisc 0.2 μm syringe filters with PTFE membranes. The filtered solutions were analyzed by HPLC, and difference method analysis was applied to determine the target removed from solution.

Columns of the materials were prepared in BioRad disposable polypropylene columns using 25 or 200 mg of sorbent. Both gravity flow and controlled flow (4 mL/min) experiments were conducted. Controlled flow was accomplished using a peristaltic pump. As with batch experiments, HPLC difference analysis was used to determine target bound. Elution from the columns was accomplished using acetonitrile or methanol. LiChrolute EN and Porapak RDX (125 – 150 μm) materials were handled identically to the sorbents prepared in house.

HPLC Analysis.

HPLC analysis was carried out on a Shimadzu High Performance Liquid Chromatography (HPLC) system with dual-plunger parallel flow solvent delivery modules (LC-20AD) and an auto-sampler (SIL-20AC) coupled to a photodiode array detector (SPD-M20A). A modification of EPA method 8330 was employed. The stationary phase was an 250 mm Altech Alltima C18 (5μm) analytical column with an isocratic 50:50 methanol:water mobile phase. A 20 μL sample injection was used with a flow rate of 1.3 mL/min. Samples solutions were in water, methanol, or acetonitrile as indicated. UV/vis detection of targets was accomplished at 254 nm.

Nitrogen sorption/TGA/XRD.

Nitrogen sorption experiments were performed on a Micromeritics ASAP 2010 at 77 K. Samples were degassed to 1 μm Hg at 100 ºC prior to analysis. Surface area was determined by use of the Brunauer-Emmett-Teller (BET) method, pore size was calculated by the Barrett-Joyner-Halenda (BJH) method from the adsorption branch of the isotherm, and total pore volume by the single point method at relative pressure (P/P_0) 0.97. Thermogravimetric analysis was performed using a TA Instruments Hi-Res 2950 Thermogravimetric Analyzer under a N_2 atmosphere; temperature was ramped 5 ºC/min to 800 ºC. Powder X-ray diffraction patterns

were obtained with a Rigaku high-resolution powder diffractometer with 18 kW CuKα radiation derived from a high-power Rigaku rotating anode X-ray generator.

Soil and Water Samples.

Soil samples were provided to us by Alan Hewitt (SERDP Project ER-1481) US Army Corps of Engineers, Engineer Research and Development Center. These samples were collected from sites at Holloman Air Force Base, Alamogordo, NM. The photo below shows the sites from which the 2000 lb bomb crater samples were collected. This was an area where a 2000 lb bomb had low-ordered (bottom of crater with man on rim) scattering Tritonal over the surface, in mainly one direction, for several 100's of meters. As seen in the pictures, the TNT (Figure 10, Panels B and C) in the Tritonal had reacted to the sun, thus leading to the formation of TNB and DNA. Some TNT had also washed from the surface during the infrequent rain events in the area leading to the formation of 2 & 4-ADNT. 2,4-DNT is also found as an impurity in the manufacturing of TNT. The samples were collected, air dried and ground, subsampled and analyzed in accordance with Method 8330B. A. Hewitt also provided well water samples taken at his home in New Hampshire.

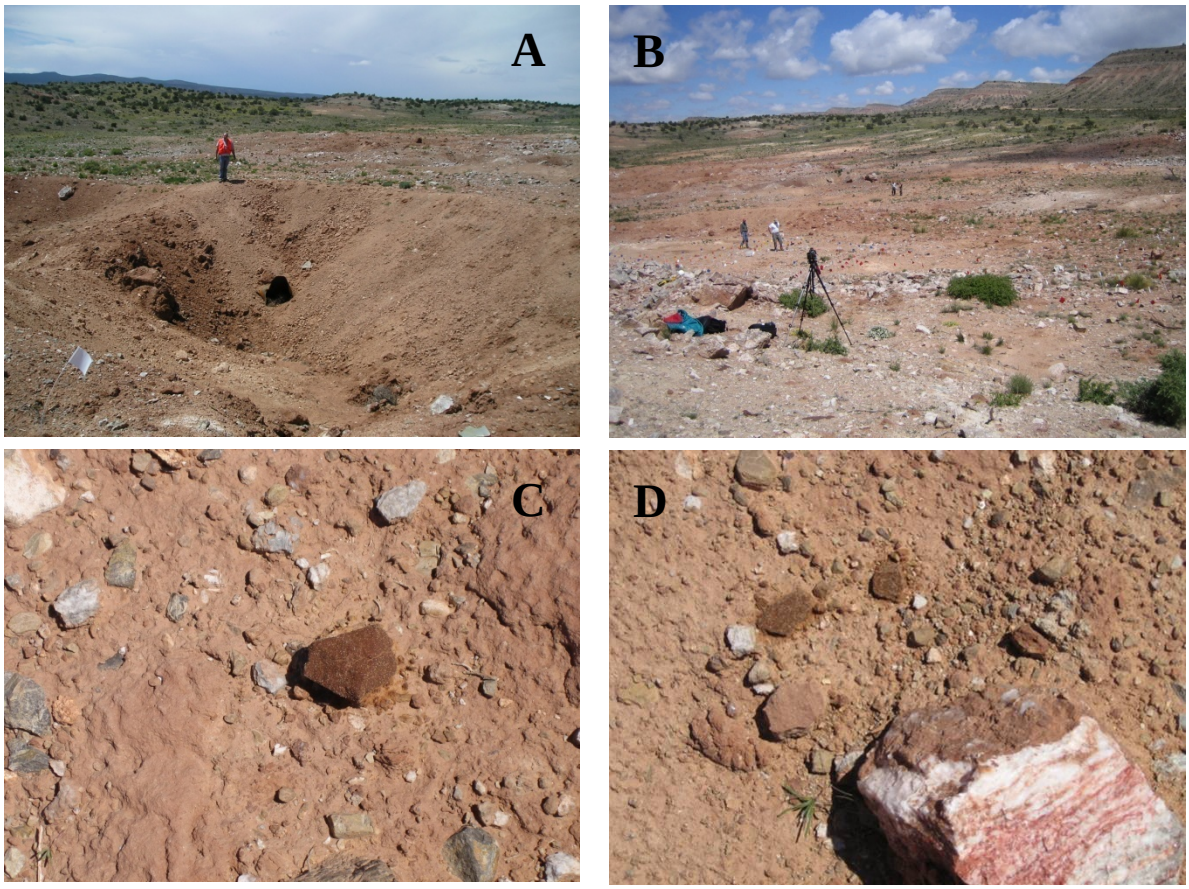

Figure 10. *Photos of soil sample collection sites on Holloman AFB.* ***A.*** *2000 lb bomb crater with low-level scattering.* ***B.*** *Wider angle view of the collection site.* ***C.*** *and* ***D.*** *These images show Tritonal in which the TNT has reacted to the sun to produce TNB and DNA.*

Kim Granzow and Michael Dale from the New Mexico Environment Department, Department of Energy Oversight Bureau provided groundwater samples taken from several springs. Bulldog Spring is a perennial spring located on Los Alamos National Laboratory. Martin, SWSC, and Burning Ground Springs are sampled biannually as part of a corrective measures study (CMS) being carried out by Las Alamos National Laboratory (CMS/CMI for Consolidated Unit 16-021©-99, the TA-16-260 Outfall).

SEM and TEM.

Samples were mounted on SEM stubs using conducting carbon tape. Sputter coating with gold under argon was accomplished using a Cressington 108 auto sputter coater for a duration of 60 sec. Scanning electron micrographs of the samples were collected using a LEO 1455 SEM (Carl Zeiss SMT, Inc., Peabody, MA). Instrument settings were as follows: tungsten filament, secondary electron detector, 20.00 kV beam voltage, 300 V collector bias, 30.00 mm aperture, 6 mm working distance. For TEM imaging, each sample was combined with absolute ethanol (Aldrich, Milwaukee, WI), agitated for 15 minutes at room temperature in a sonic bath, deposited onto a holey carbon grid (200 mesh copper, SPI, West Chester, PA), and viewed under an energy filtering transmission electron microscope (LIBRA 120 EFTEM, Carl Zeiss SMT, Peabody, MA) operated at 120kV. Zero Loss, brightfield, EFTEM images were captured on a bottom-mounted, digital camera (KeenView, Olympus SIS, Montvale, NJ).

Results and Accomplishments

Phase I. Materials Development

For Phase I of this project, the primary focus was on the synthesis and evaluation of the mesoporous materials and their capacity to concentrate energetic materials from groundwater. Materials optimization consisted of studies to optimize the desired properties, i.e. target capacity, binding affinity and selectivity, and elution characteristics. These optimizations included looking at variations on the imprint template as well as evaluating adjustments to the synthesis protocol including alternative precursors, alternate surfactant to precursor (bridging group) ratios, template imprint molecule variations, and hydrothermal treatments.

Co-condensation Variants.

The exceptional binding characteristics of the DEB-bridged materials described previously lead to consideration of co-condensation approaches for the generation of materials with improved structural characteristics. The goal was to generate high surface area materials with uniform pores which demonstrated binding affinities approaching those observed in the 100% DEB materials. In addition, it was expected that material structures with uniform pores would be more susceptible to the imprinting process and would, therefore, offer advantages in selectivity and tunability. With these points in mind, several materials, both imprinted and non-imprinted, were synthesized with varying ratios of DEB to BTE (Table 1). As expected, incorporation of the large organic bridging group (DEB) was found to disrupt the structure of the resulting materials. This is evidenced by the decrease in surface area, pore diameter, and pore volume as the DEB precursor was increased from 0 to 100% of the total precursor used (Table 1). At 40% DEB (M-60:40) a transition from mesoporous (pore diameters 20 to 500 Å according to the IUPAC definition) to microporous (pore diameters less than 20 Å) was noted. All materials

attained equilibrium adsorption in less than 30 min. Materials with uniform mesopores, such as M-70:30, were found to reach equilibrium adsorption in less than 3 minutes.

The binding capacity and selectivity for each material were evaluated through a combination of experiments. First, materials were exposed to single analyte solutions (including TNT, pNP, and pCr) overnight on a rotisserie shaker in order to determine the total binding capacity for each analyte under identical conditions. HPLC difference method was used to determine the amount of target bound from each solution (Table 1). As expected, the binding capacity of M-100:0 (100% BTE) was low (0.34μg/m^2 for TNT). The binding capacity for all three analytes increased with increasing DEB incorporation with the capacity for TNT reaching a value of 16.3 μg/m^2 for the 100% DEB material (M-0:100). The binding capacity for pNP and pCr remained relatively low for materials with 50% or less DEB incorporated (Figure 11). The M-0:100 material, however, bound pCr equivalent to 62% and pNP equivalent to 21% of the TNT bound. Because TNT was the target of interest, these results would tend to indicate a significant degree of undesirable binding.

As TNT was the target of interest for these studies, competitive binding in a three component mixture (TNT, pNP, and pCr each at 22 μM) was used to evaluate the tendency for TNT binding over that of other compounds of similar structure. While the binding of TNT by M-100:0 and M-90:10 was not impacted by the presence of pCr and pNP in the sample, the other materials showed a reduction in TNT bound per surface area when the target was presented in the mixed sample (Table 1). The pCr bound from the mixture was less than that bound from single analyte solutions for the materials while the binding of pNP was only slightly impacted. The exception was M-0:100 for which the binding of pNP was reduced by 72% and that of pCr by 85% in the mixed sample. This result reflects the dramatically increased capacity for the binding of these analytes from single target solutions by M-0:100.

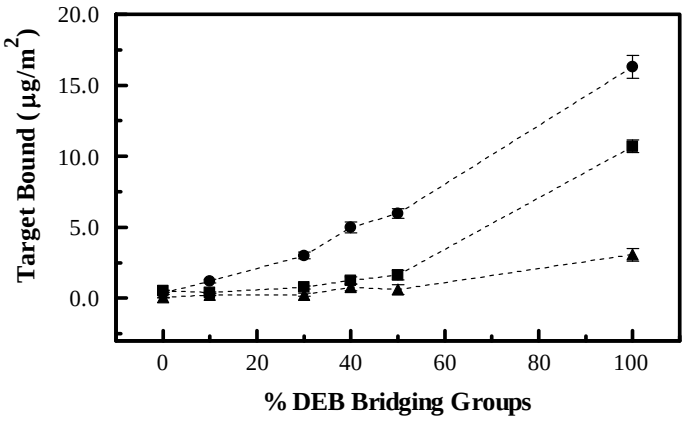

Figure 11. *Bridging group variations. The amount of target (TNT (●), pCr (■), pNP (▲)) bound by the materials increases as the percentage of DEB used during synthesis is increased. All target concentrations were 22 μM; data presented here is for adsorption from single target samples. The curves presented represent the average of three measurements.*

Table 1. *Co-condensate materials characteristics and binding capacities.*

						Mixed Samples‡					
Material	% DEB†	% mod-Brij@	Surface Area (m^2/g)	Pore Volume (cm^3/g)	Pore Diameter (Å)	TNT*	TNT*	pNP*	pNP*	pCr*	pCr*
M-100:0	0	0	1180	1.07	38	0.34(0.02)	0.39(0.03)	0.04(0.03)	0.09(0.03)	0.55(0.03)	0.39(0.03)
M-100:0 Imp	0	12.5	1157	1.07	39	0.32(0.06)	0.41(0.07)	0.00(0.00)	0.03(0.01)	0.60(0.05)	0.29(0.02)
M-90:10	10	0	1071	0.75	28	1.19(0.04)	1.23(0.04)	0.24(0.04)	0.23(0.01)	0.40(0.02)	0.28(0.02)
M-90:10 Imp	10	12.5	1077	0.78	30	1.03(0.03)	1.18(0.03)	0.11(0.03)	0.00(0.00)	0.37(0.01)	0.19(0.02)
M-75:25	25	0	1056	0.63	22						
M-75:25 Imp	25	12.5	1075	0.64	23						
M-70:30	30	0	1004	0.56	21	3.01(0.05)	2.07(0.05)	0.24(0.02)	0.22(0.03)	0.77(0.01)	0.55(0.03)
M70:30 Imp	30	12.5	1095	0.60	22	2.97(0.02)	3.42(0.04)	0.35(0.03)	0.10(0.04)	0.74(0.05)	0.41(0.01)
M-60:40	40	0	922	0.52	<20	4.98(0.04)	3.49(0.05)	0.78(0.01)	0.73(0.04)	1.25(0.03)	0.90(0.07)
M-60:40 Imp	40	12.5	957	0.52	<20	4.97(0.05)	2.64(0.05)	0.75(0.01)	0.22(0.04)	1.32(0.03)	0.57(0.05)
M-50:50	50	0	813	0.46	<20	5.98(0.07)	4.07(0.04)	0.60(0.03)	0.73(0.03)	1.65(0.04)	1.14(0.02)
M-50:50 Imp	50	12.5	847	0.44	<20	5.90(0.05)	3.66(0.07)	1.59(0.05)	0.34(0.03)	1.69(0.02)	0.72(0.02)
M-0:100	100	0	356	0.20	<20	16.30(0.10)	12.09(0.10)	3.07(0.03)	0.86(0.05)	10.71(0.05)	1.65(0.03)
M-0:100 Imp	100	12.5	317	0.18	<20	19.36(0.08)	12.08(0.09)	3.03(0.02)	0.98(0.03)	12.93(0.06)	1.37(0.04)

** Amount of analyte bound in μg/ m^2. The number in parenthesis indicates the standard deviation of three measurements.*
@ Indicates the percentage of DNB-modified Brij®76 used to imprint the material.
† Indicates the percentage of DEB precursor used during synthesis.
‡ Gray shaded columns indicate the use of mixtures of targets.
All targets present at 22 μM.

Imprinting the co-condensates through substitution of 12.5% DNB-Brij imprint molecule for Brij®76 was not found to significantly alter the materials characteristics (Table 1). The effectiveness of imprinting in the co-condensates was evaluated by comparing the performance of the imprinted materials to that of the non-imprinted materials. Both single and multiple target experiments were employed. The adsorption of targets from mixtures must be considered with care due to the potential for solute-solute interactions. In addition, the relative affinity of each target for the available adsorption sites may vary resulting in more complicated adsorption behavior. Binding of the targets from single analyte solutions was similar for the imprinted and non-imprinted materials when less than 50% DEB bridging group was incorporated. An increase in TNT capacity was noted upon imprinting of M-0:100 (M-0:100 Imp; Table 1, based on single analyte solutions). The total pNP and pCr binding from single analyte solutions was not significantly impacted upon imprinting of the materials against the dinitrobenzene (DNB) analog (Table 1).

The effect of imprinting was more clearly observed when co-condensate materials were incubated with the mixture of TNT, pNP, and pCr. While M-100:0 and M-90:10 showed no difference in adsorption of TNT whether from the mixture or single analyte solution, M-100:0 Imp, M-90:10 Imp, and M-70:30 Imp showed a slight enhancement (~15%) in TNT absorption (Figure 12). This was in contrast to the decrease in TNT absorption seen with the non-imprinted materials upon incubation with the mixed sample. M-60:40 Imp, M-50:50 Imp, and M-0:100 Imp did not demonstrate enhanced TNT adsorption due to imprinting. In fact, these materials bound less TNT from the mixed sample as compared to single analyte samples (Figure 12). The involvement of non-specific binding sites may account for this behavior but the available data did not allow a conclusive determination. For all cases, the observed reduction in pCr and pNP binding from the mixed sample as compared to single analyte samples was greater for the imprinted materials than for the non-imprinted materials. This tended to indicate an enhancement in TNT selectivity upon imprinting. These results also indicated that the effectiveness of imprinting varied with percentage of incorporated DEB.

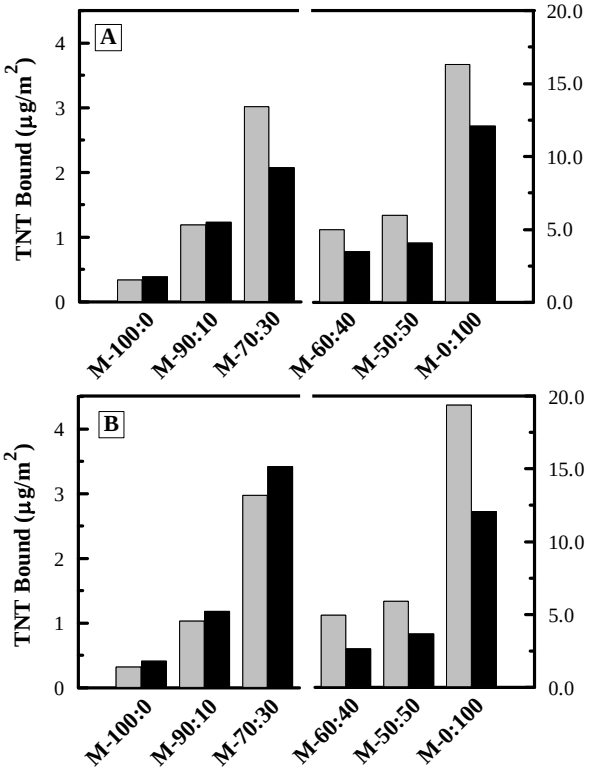

Figure 12. *Bridging group variations. The amount of target (TNT (●), pCr (■), pNP (▲)) bound by the materials increases as the percentage of DEB used during synthesis is increased. All target concentrations were 22 µM; data presented here is for adsorption from single target samples. The curves presented represent the average of three measurements.*

Imprint Variations.

In order to determine the optimal imprint molecule concentration, M-70:30 materials were synthesized with 12.5%, 25%, 50%, and 100% of the Brij®76 surfactant replaced by DNB-Brij. This replacement was not found to strongly impact the surface area or total pore volume of the M-70:30 Imp, Imp 25, or Imp 50 materials (Table 2). The M-70:30 Imp 100 material showed significantly reduced surface area as compared to the other materials. The average pore diameter of the materials was found to increase with increasing imprint molecule incorporation from 21 Å (no imprint) to 31 Å (100% modified Brij®76). The changes in pore diameter appeared to be consistent with an alteration in the average length of the surfactant molecule employed.

Single analyte and mixed target solutions were again employed to determine binding capacities and to obtain estimates of the selectivity for TNT binding over that of similar molecules. Though a consistently increasing or decreasing trend was expected for this series of materials, this was not observed (Table 2). In fact, M-70:30 Imp 25 consistently bound less target than the other materials indicating some disruption of imprinting process. M-70:30 Imp 100 demonstrated marked improvement in TNT and DNT binding capacity as well as a slight enhancement in RDX binding capacity. With the exception of M-70:30 Imp 100, pNP, pCr, and RDX binding by the M-70:30 materials was minimal when compared to TNT binding. The addition of glycine (100 μM) to samples containing 22 μM TNT did not impact the adsorption of TNT by any of the M-70:30 materials (data not shown).

The imprint materials were incubated with several mixed sample solutions: TNT, pCr, and pNP (Solution A); TNT and DNT; TNT and RDX; and DNT and RDX (all analytes at 22 μM). Evaluation of target binding from Solution A indicated that the slight enhancement in TNT binding demonstrated by M-70:30 Imp (above) was also obtained for M-70:30 Imp 25 and M-70:30 Imp 50. It was not the case for M-70:30 Imp 100 where a significant decrease in TNT binding was observed when present in the mixture (Table 2). Although the M-70:30 Imp products did not exhibit meso-structures with long-range order that could be determined by XRD (contrast with M-100:0 products), most of them had uniform pore sizes as determined by nitrogen adsorption pore size distributions. These materials also yielded single low angle XRD reflections consistent with mesoporous materials that have uniform pore dimensions but disordered packing.[26; 27] M-70:30 Imp 100 was notably different. It did not show a XRD reflection (Figure 13) and produced a broader, less sharply defined nitrogen adsorption pore size distribution compared to the other M-70:30 Imp variants (Figure 14). The nitrogen sorption isotherm (Figure 15) was distorted in shape with a wider hysteresis between the adsorption and desorption branches compared to the other variants which displayed type IV/type I isotherms common to mesoporous materials with uniform pore sizes ca. 20 Å. These distinct structural differences likely resulted in the unique behavior of M-70:30 Imp 100.

The DNT binding capacity of the M-70:30 materials was found to be comparable to that of the TNT. DNT was used as an alternative target in these studies because of the structural similarity to the imprint molecule and to TNT. The presence of DNT was found to compete for sites that bound TNT more strongly in M-70:30 Imp 100 than in the others with M-70:30 Imp showing the least impact (Table 3). Similarly, the presence of TNT had the least impact on DNT binding in M-70:30 Imp. The presence of RDX had little effect on either DNT or TNT binding in this material while strong competition between all three analytes was noted for M-70:30 Imp 100. M-70:30 Imp 25 showed the highest selectivity against RDX but the lowest total binding capacity for all targets.

Table 2. *Imprint variant materials characteristics and binding capacities.*

					Mixed Samples†							
Material	**% mod-Brij@**	**Surface Area (m^2/g)**	**Pore Volume (cm^3/g)**	**Pore Diameter (Å)**	**TNT***	**TNT***	**pNP***	**pNP***	**pCr***	**pCr***	**DNT***	**RDX***
M-70:30	0	1004	0.56	21	3.01(0.05)	2.00(0.05)	0.24(0.02)	0.22(0.03)	0.77(0.01)	0.54(0.03)	2.62(0.06)	0.87(0.03)
M-70:30 Imp	12.5	1095	0.60	22	2.97(0.02)	4.05(0.04)	0.35(0.03)	0.11(0.04)	0.74(0.05)	0.42(0.01)	3.05(006)	0.70(0.03)
M-70:30 Imp 25	25	977	0.59	23	2.13(0.04)	3.19(0.07)	0.33(0.03)	0.22(0.05)	0.63(0.03)	0.42(0.01)	2.55(0.05)	0.51(0.05)
M-70:30 Imp 50	50	1028	0.63	26	2.79(0.08)	3.80(0.05)	0.31(0.02)	0.13(0.02)	0.71(0.03)	0.33(0.02)	2.95(0.06)	0.64(0.04)
M-70:30 Imp 100	100	707	0.59	31	5.17(0.10)	2.44(0.10)	0.45(0.02)	0.23(0.02)	1.38(0.02)	0.51(0.04)	5.25(0.07)	1.17(0.05)

**Amount of analyte bound in μg/m^2. The number in parenthesis indicates the standard deviation of three measurements.*
@ Indicates the percentage of DNB-modified Brij®76 used to imprint the material.
†Mixed samples are indicated by gray shading.
All targets present at 22 μM.

Table 3. *Targets bound from multi-target samples.*

Material	TNT*			DNT*			RDX*		
	TNT	TD[†]	TR[‡]	DNT	TD[†]	DR[&]	RDX	TR[‡]	DR[&]
M-70:30	3.01(0.05)	2.60(0.10)	2.95(0.09)	2.62(0.06)	2.06(0.09)	2.79(0.06)	0.87(0.03)	0.73(0.02)	0.47(0.03)
M-70:30 Imp	2.97(0.02)	2.81(0.10)	2.61(0.07)	3.05(0.06)	3.01(0.07)	2.95(0.08)	0.76(0.03)	0.57(0.05)	0.76(0.04)
M-70:30 Imp 25	2.13(0.04)	1.84(0.13)	1.97(0.10)	2.55(0.05)	2.05(0.08)	1.99(0.07)	0.51(0.05)	0.34(0.03)	0.04(0.03)
M-70:30 Imp 50	2.79(0.08)	2.32(0.11)	2.54(0.09)	2.95(0.06)	2.52(0.08)	2.77(0.07)	0.64(0.04)	0.50(0.03)	0.43(0.01)
M-70:30 Imp 100	5.17(0.10)	4.07(0.09)	4.38(0.11)	5.25(0.07)	4.43(0.06)	4.85(.010)	1.17(0.05)	0.85(0.02)	0.91(0.03)

** Amount of analyte bound in $\mu g/m^2$. The number in parenthesis indicates the standard deviation of three measurements. Single target samples contained 22 μM of the indicated compound.*

[†] Sample contained 22 μM TNT and DNT.

[‡] Sample contained 22 μM TNT and RDX.

[&]Sample contained 22 μM DNT and RDX.

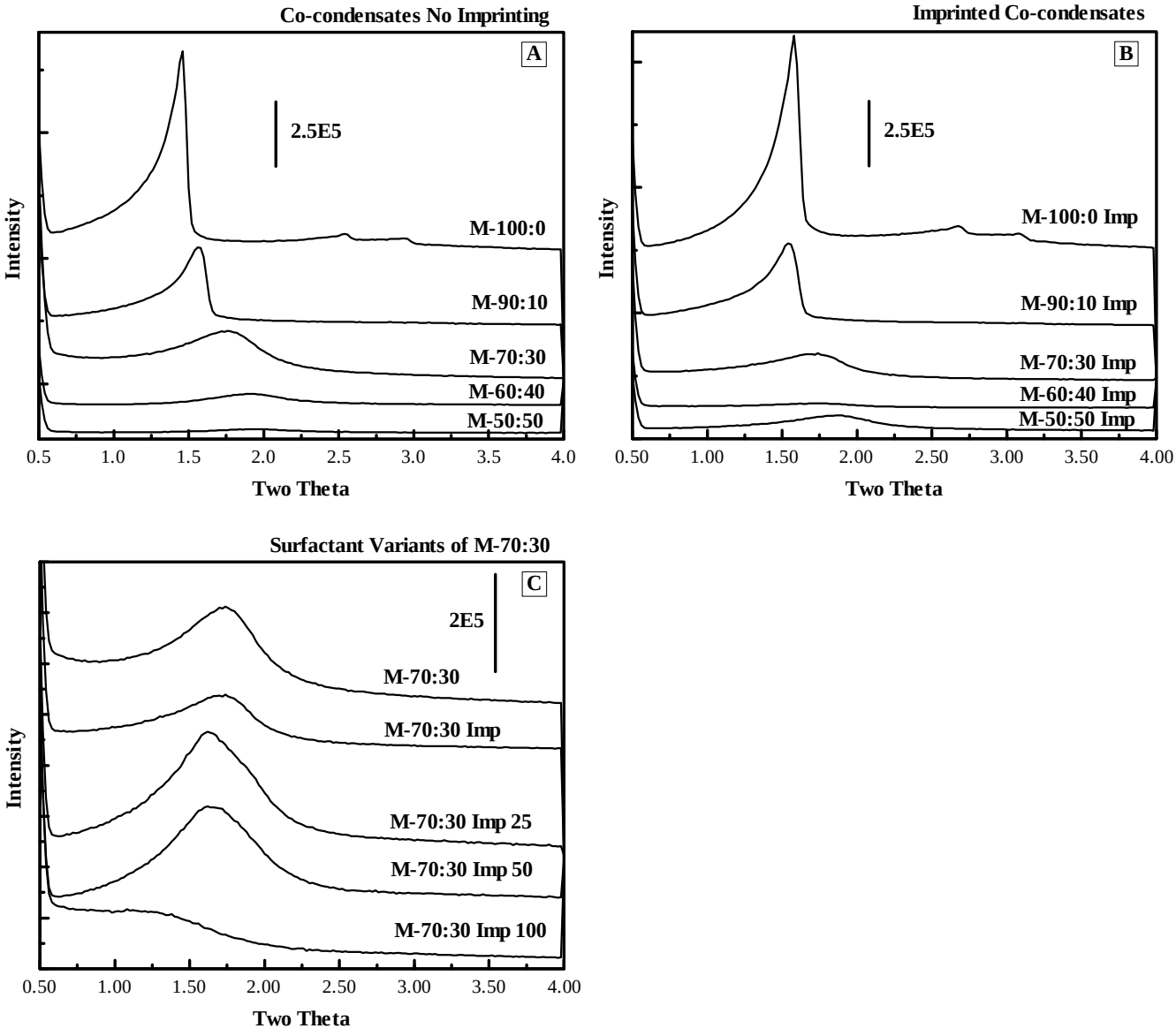

Figure 13. *XRD spectra for the materials synthesized: co-condensates with varying DEB concentrations (Panel A); co-condensates with varying DEB concentrations imprinted using 12.5% DNB-modified Brij®76 and 87.5% Brij®76 (Panel B); 70% BTE: 30% DEB co-condensates imprinted using varying ratios of Brij®76 to modified Brij®76 (Panel C). XRD spectra for 100% DEB materials are not presented due to the lack of features. The imprinted and non-imprinted co-condensate materials (Panels A and B) show similar features. It is interesting to note that the material synthesized using 100% modified Brij®76 is significantly less ordered than the other M-70:30 materials.*

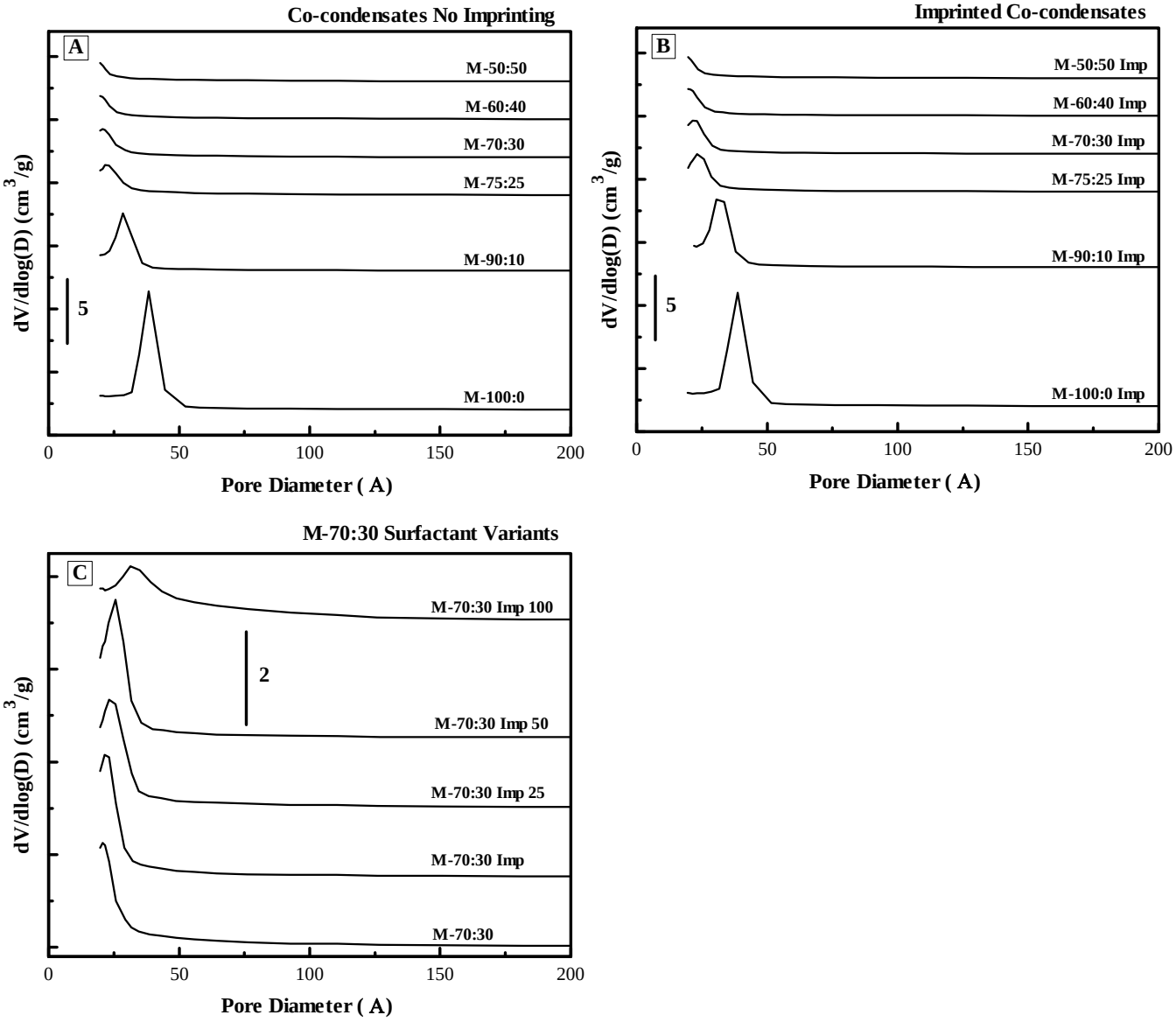

Figure 14. *Pore diameter distributions for each of the materials synthesized: co-condensates with varying DEB concentrations (Panel A); co-condensates with varying DEB concentrations imprinted using 12.5% DNB-modified Brij®76 and 87.5% Brij®76 (Panel B); 70% BTE: 30% DEB co-condensates imprinted using varying ratios of Brij®76 to modified Brij®76 (Panel C). A transition from mesoporous to microporous is observed as the percentage of DEB used is increased (Panels A and B). The average pore diameter increases as the percentage of modified Brij®76 incorporated is increased (Panel C).*

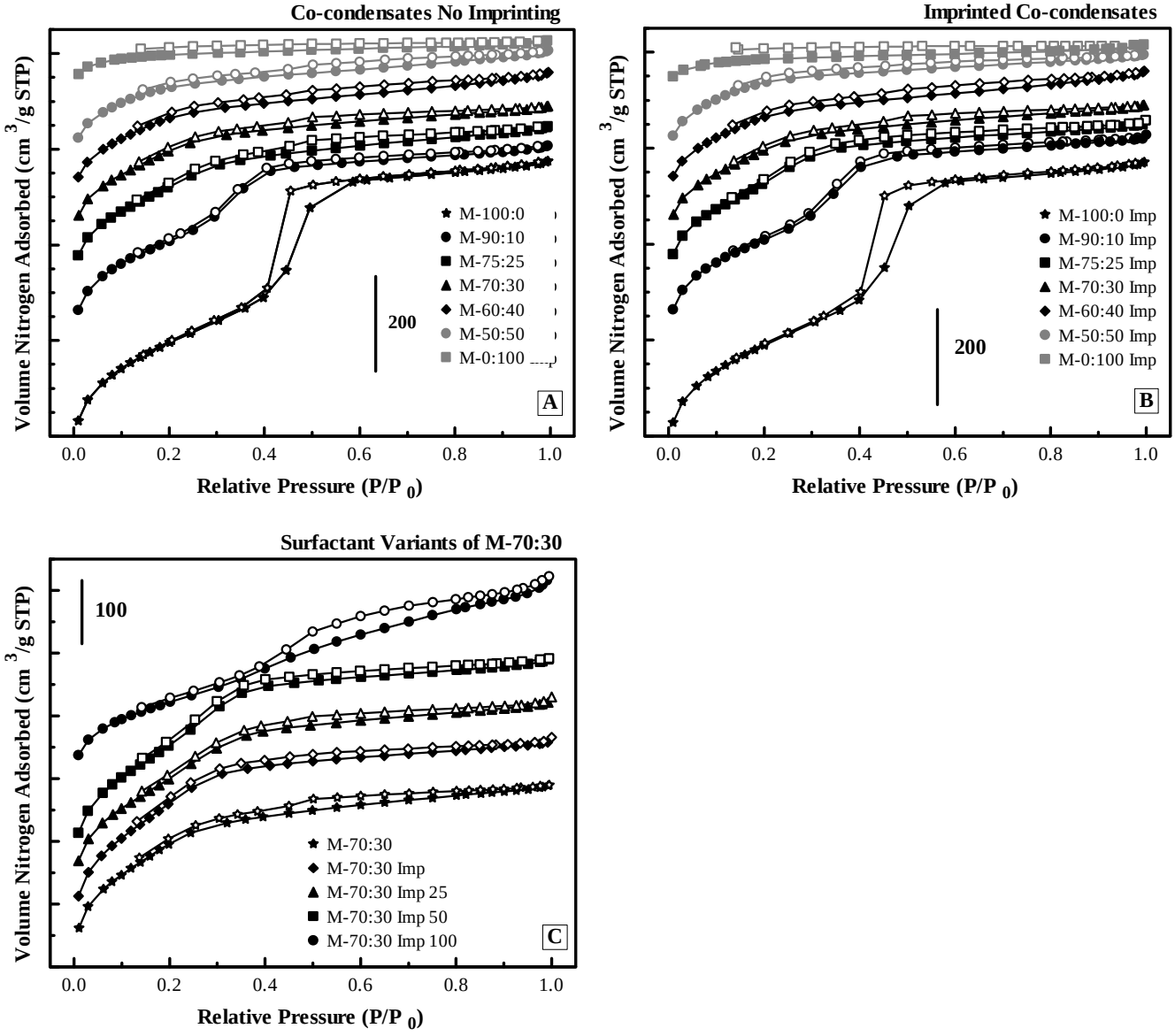

Figure 15. *Nitrogen sorption isotherms for each of the materials synthesized: co-condensates with varying DEB concentrations (Panel A); co-condensates with varying DEB concentrations imprinted using 12.5% DNB-modified Brij®76 and 87.5% Brij®76 (Panel B); 70% BTE: 30% DEB co-condensates imprinted using varying ratios of Brij®76 to modified Brij®76 (Panel C). All isotherms are Type IV or indicate transition from Type I to Type IV.*

In order to obtain a number indicative of affinity, linear fits for the double reciprocal form of the isotherms presented in Figure 16 were generated (Figure 17; units converted to μg/m2 vs. μg). The fitting parameters obtained were used to determine the parameters of the Langmuir-Freundlich model isotherms of the form:

$$q = \frac{q_s k[L]^n}{1 + k[L]^n} \qquad \textit{(Equation 1)}$$

which allowed for calculation of q_s as the inverse of the *y*-intercept and *k* as the ratio of the *y*-intercept to the slope when *n* was held at a constant value of 1 (Table 4). Here, q_s is the saturation capacity; [L] is the concentration of unbound target, *q* is the bound target; and *n* is the heterogeneity index. The Langmuir-Freundlich model is a generalization of the Langmuir model used to account for surface heterogeneity (non-identical sites).([28; 29]) The Langmuir model, representing a general binding isotherm for identical, independent binding sites possessing an association constant of *k* for the specified ligand, is recovered for the case when the heterogeneity index is unity. Good fitting parameters for q_s and *k* were obtained when the heterogeneity index was fixed at unity. Accurate values of *n* could not be determined due to the limited range of concentrations available from the adsorption experiments. The range was limited due to two factors: First, TNT stocks are received as 1 mg/ml solutions in acetonitrile. In order to prevent alterations in target adsorption owing to adsorbent wetting conditions and target solubility, the final acetonitrile concentration in samples was kept to a minimum and held constant. The other factor was the restraints implicit in the use of HPLC for determination of concentration. The range of concentrations tested in these studies was achieved by varying the amount of adsorbent while holding the TNT concentration constant. Based on this isotherm units of inverse μg for *k* and μg/m^2 for q_s were obtained These units did not allow for comparison to association constants in solution, for example, but they did provide a metric for comparison of the various materials to each other.

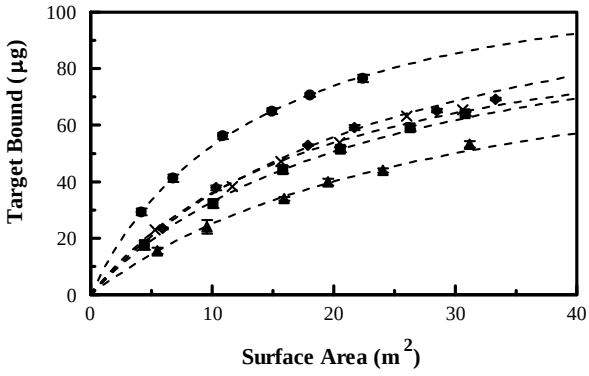

Figure 16*. Binding isotherms. TNT binding isotherms and the corresponding curve fits are presented for each of the surfactant variants: M-70:30 (**x**), M-70:30 Imp (♦), M-70:30 Imp 25 (▲), M-70:30 Imp 50 (■), M-70:30 Imp 100 (●). The TNT concentration was 22 μM for all experiments. Curve fit parameters are provided in Table 4.*

The method of Ockrent [30] and Weber [31] for prediction of the adsorption of two targets provides another method for determining the heterogeneity of binding sites. This technique is based on an extension of the Langmuir model and is analogous to the relationship proposed for mixed-gas adsorption. The following relationship is reported:

$$\frac{n_1^{mix}}{n_1^{single}} = 1 - \frac{n_2^{mix}}{n_2^{single}} \qquad \textit{(Equation 2)}$$

where n_1^{mix} is the concentration of target 1 absorbed from the mixture of target 1 and target 2 and n_1^{single} is the concentration of target 1 adsorbed from the single analyte solution when the total

initial target and adsorbent concentrations are fixed at the same value for all solutions. Similarly for n_2, "mix" indicates the two target solution and "single" indicates the single analyte solution. Deviation from this relationship indicates heterogeneity; the greater the deviation the larger the diversity of sites. When this relationship was applied to the data obtained using the imprint variants, M-70:30 Imp 25 was found to display the strongest deviation from the expression (Equation 2). The other five materials performed similarly to one another with deviations of less than 0.15 from the linear function (Tables 5 and 6).

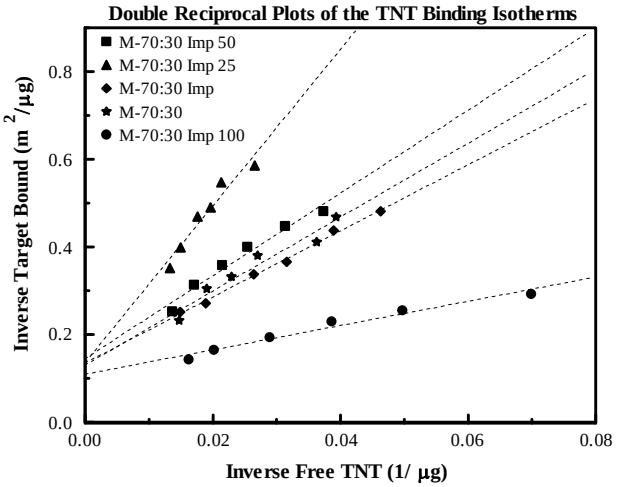

Figure 17. *Double reciprocal form of the TNT binding isotherms presented in Figure 14. The double reciprocal linearization was used to generate fitting parameters for each of the materials (Table 4). These parameters were used to calculate association constants for the materials to facilitate comparisons between these and other materials.*

Table 4. *Fit parameters and calculated constants from TNT binding isotherms.*

	slope (m^2)	*y*-intercept ($m^2/\mu g$)	q_s ($\mu g/m^2$)	k (μg^{-1})
M-70:30	8.44	0.1305	7.66	0.0155
M-70:30 Imp	7.54	0.135	7.41	0.0179
M-70:30 Imp 25	17.86	0.1362	7.34	0.0076
M-70:30 Imp 50	9.45	0.1451	6.89	0.0154
M-70:30 Imp 100	2.77	0.1097	9.12	0.0396

The calculated association constants further illuminated an unexpected trend in the materials (Table 4). While M-70:30 Imp 100 was superior to the other materials in terms of saturation capacity and association constant, the saturation capacity of the materials decreased with increasing imprint molecule concentration from 0 to 50%. M-70:30 Imp 25 demonstrated the weakest association constant. M-70:30 was found to have the second strongest association constant followed by nearly identical capacities for M-70:30 Imp and M-70:30 Imp 50. These trends may have resulted from surfactant partitioning during the synthesis of the materials. If the DNB-Brij and Brij®76 tended to separate within the micelles, transitions from Brij®76 regions to DNB-Brij regions would result. These transitions could cause disruption of the pore wall structure upon condensation, thereby reducing the functional surface area of the materials. The greatest impact of this effect would be observed for micelles with the highest number of transitions; there would be none for M-70:30 Imp 100 or M-70:30. M-70:30 Imp used a very low concentration of DNB-Brij, so formation of separate Brij®76/DNB-Brij regions would be

unlikely. The high concentration of DNB-Brij in M-70:30 Imp 50 should result in formation of large regions of DNB-Brij within the micelles and, therefore, the number of transitions would be reduced as compared to M-70:30 Imp 25.

Table 5. *Targets bound from mixed samples.*

Material	**TNT***			**DNT***			**RDX***		
	TNT	TD[†]	TR[‡]	DNT	TD[†]	DR[&]	RDX	TR[‡]	DR[&]
M-70:30	3.01	1.64	1.77	2.62	1.40	1.55	0.87	0.31	0.30
M-70:30 Imp	2.97	1.65	1.73	3.05	1.39	1.54	0.70	0.29	0.29
M-70:30 Imp 25	2.13	1.12	1.12	2.55	0.99	1.06	0.51	0.00	0.12
M-70:30 Imp 50	2.79	1.58	1.71	2.95	1.34	1.50	0.64	0.27	0.26
M-70:30 Imp 100	5.17	2.73	2.96	5.25	2.33	2.61	1.17	0.47	0.47

** Amount of analyte bound in μg/m^2; all samples contained 22 μM target.*

[†] *Sample contained 11 μM TNT and DNT.*

[‡] *Sample contained 11 μM TNT and RDX.*

[&] *Sample contained 11 μM DNT and RDX.*

Table 6. *Heterogeneity as indicated by ratios of target adsorption from single and multi-target solutions.*

Material	**TNT and DNT**		**TNT and RDX**		**DNT and RDX**	
	TNT(TD)/TNT(1)*	DNT(TD)/DNT(1)	TNT(TR)/TNT(1)	RDX(TR)/RDX(1)	DNT(DR)/DNT(1)	RDX(DR)/RDX(1)
M-70:30	0.54	0.46	0.59	0.35	0.59	0.35
M-70:30 Imp	0.56	0.54	0.58	0.41	0.51	0.42
M-70:30 Imp 25	0.52	0.61	0.52	0.00	0.41	0.23
M-70:30 Imp 50	0.57	0.55	0.61	0.42	0.51	0.41
M-70:30 Imp 100	0.53	0.56	0.57	0.40	0.50	0.40

** Ratio of target adsorbed from multi-target solution to that adsorbed from single target solution from Table 5.*

(1) indicates single target solution; TD, TR, and DR are two-target solutions as defined in Table 5.

Hierarchical Materials.

Having determined the combination of characteristics that produce a material which has the structural and binding characteristics that are desirable, we wanted to address the back pressure issues which have presented difficulties to the application of these types of materials in the past. Mixing of these materials with sand or other materials of a controlled particle size has been described. This allowed for application in column formats; however, this reduces the capture surface area in the column. In addition, the PMO materials will eventually compact at the end of the column resulting in the same back pressure issues. The back pressures observed result from several factors: the particle sizes in the PMO powders are small allowing for dense packing within the column; there may be poor interconnectivity between the pores throughout a given particle; the pore sizes within the particles are on the order of 30 Å. We determined that, using a variation on the materials synthesis, we could generate larger pores to provide reduced pressure and increased connectivity and flow while maintaining the meso-structure which provides the desired high concentration of binding sites. Figure 18 shows SEM and TEM images of one such material.

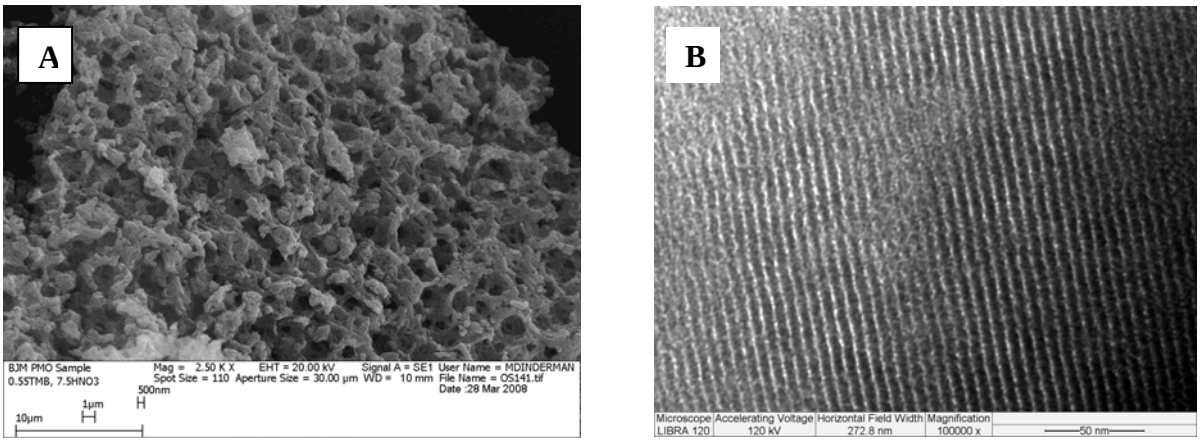

Figure 18. ***A.*** *SEM image of a hierarchical material showing the macro-strcuture. This is a 50:50 DEB:BTE material synthesized with no imprint.* ***B.*** *TEM image of the hierarchical material showing the meso-structure.*

XRD spectra of the hierarchical materials indicate that it is possible to increase the concentration of DEB in the materials as compared to the mesoporous materials (above) while maintaining a higher degree of order. This is indicated both by the sharp profile of the primary reflection as well as by the presence of additional reflections in the spectrum (Figure 19). A comparison of the pore size distributions indicates larger mesopores within the hierarchical materials as well (Figure 20). The nitrogen sorption analysis yielded type IV/type I isotherms common to mesoporous materials with uniform pore sizes (Figure 21).

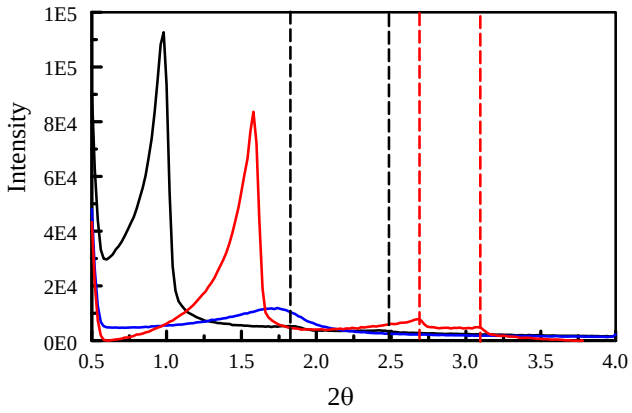

Figure 19. *XRD spectra of the 12.6% Imp 50:50 DEB:BTE hierarchical material (black), M-70:30 Imp (blue), and M-100:0 (red). Vertical lines show the positions of additional reflections.*

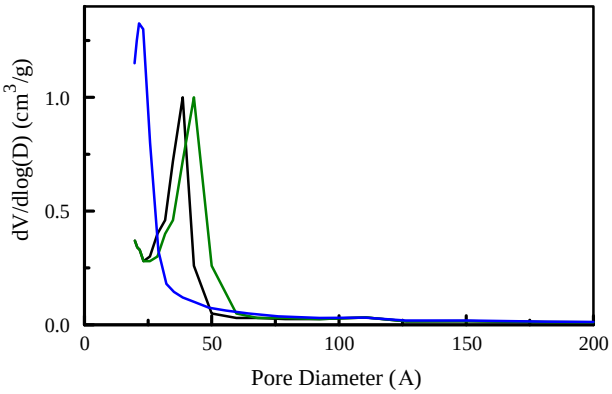

Figure 20. *Pore size distributions for the 12.6% Imp 50:50 DEB:BTE hierarchical material (black), the hierarchical P10 (green), and M-70:30 Imp (blue).*

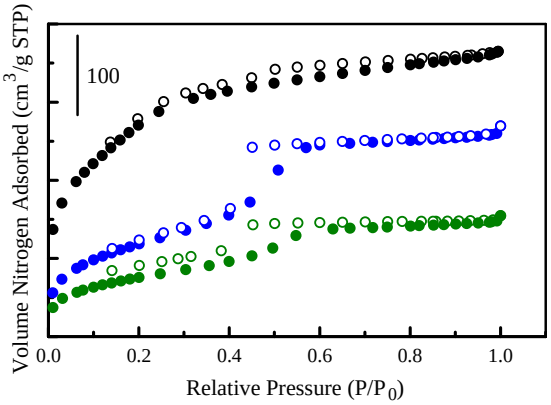

Figure 21. *Nitrogen sorption (solid)/desorption (open) isotherms for the 12.6% Imp 50:50 DEB:BTE hierarchical material (black), the hierarchical P10 (green), and M-70:30 Imp (blue).*

In order to optimize the synthesis of these types of materials, the mesitylene and nitric acid concentrations as well as the precursor ratios had to be optimized. Optimizing this synthesis required an iterative approach. Holding the precursor ratio and acid concentrations constant, the mesitylene concentration was varied. From this data, a mesitylene (TMB) concentration was selected and the precursor ratio was varied (still holding the acid concentration constant). Table 7 shows the impact on structural characteristics when the DEB precursor concentration is increased from 50%. Because of the dramatic loss in surface area and pore volume for higher concentrations and the fact that a well ordered structure was obtained at a ratio of 50:50, we sought to optimize the other aspects of the synthesis using a DEB:BTE ratio of 50:50. Table 8

shows the impact of varying the nitric acid concentration used during synthesis. When 7.5 g of nitric acid was used, the surface area, pore volume, and pore diameter were maximized. At this point, the mesitylene concentration was again varied. Table 9 shows the impact of increasing concentrations of mesitylene during synthesis. On the basis of these results, the protocol for synthesis of the 50:50 DEB:BTE hierarchical materials was fixed to include 0.55 g mesitylene and 7.5 g 0.1 M nitric acid. Imprinting these materials with varying ratios of Pluronic P123 to modified P123 was also evaluated. Materials generated with 20% imprint template were found to bind only 64% of the TNT bound by materials synthesized using 12.6% imprint template. Materials which were not imprinted bound 74% of the TNT bound by the imprinted (12.6%) material.

Table 7. Structural characteristics for varying DEB to BTE ratios in the hierarchical materials.

BTE:DEB	BET surface area (m^2/g)	Pore volume (cm^3/g)	Pore diameter (Å)
50:50	335	0.301	43
25:75	69	0.0626	39
0:100	2	-	-

Here the total precursor was held constant at 7.84 mmol. All syntheses used 1.9 g Pluronic P23 0.3 g mesitylene, and 6.07 g 0.1 M HNO_3.

Table 8. Structural characteristics for varying nitric acid concentrations in the hierarchical materials.

Mass HNO_3 (g)	BET surface area (m^2/g)	Pore volume (cm^3/g)	Pore diameter (Å)
6.07	375	0.336	43
6.5	431	0.448	57
7.0	257	0.323	47
7.5	434	0.480	56
8.5	434	0.478	50

Here the total precursor was 7.84 mmol at a 50:50 DEB:BTE ratio. All syntheses used 1.9 g Pluronic P123 and 0.3 g mesitylene.

Table 9. Structural characteristics for varying mesitylene concentrations in the hierarchical materials.

Mass TMB (g)	BET surface area (m^2/g)	Pore volume (cm^3/g)	Pore diameter (Å)
0.35	433	0.485	57
0.4	457	0.430	44
0.5	455	0.460	50
0.55	456	0.483	49
0.6	436	0.490	56

Here the total precursor was 7.84 mmol at a 50:50 DEB:BTE ratio. All syntheses used 1.9 g Pluronic P123 and 7.5 g 0.1 M HNO_3.

Imprinting the hierarchical materials was found to enhance their binding capacity as well as selectivity. Figure 22 shows plots generated based on *Equation 2* (above). Here, stronger

deviation from the straight line indicates more heterogeneity in the sites involved in binding the two targets. In the material that was not imprinted, the TNT, DNT, RDX, and p-cresol were all found to bind to similar sites. In both imprinted materials, the sites to which p-cresol bound were decidedly distinct from those to which TNT bound while DNT and RDX were bound by similar sites to those occupied by TNT.

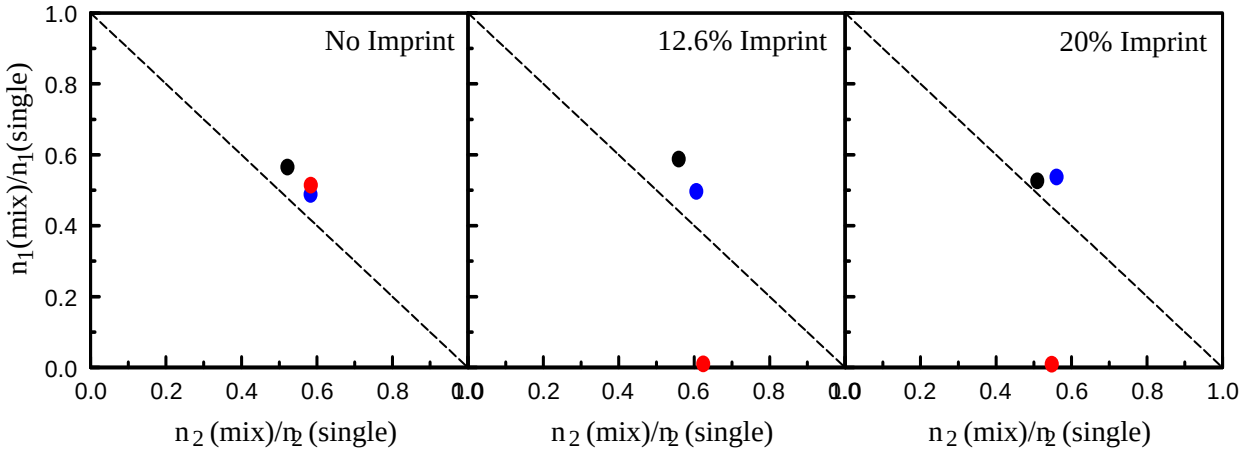

Figure 22. *Homogeneity plots generated based on Equation 2 for three 50:50 BTE:DEB hierarchical materials and three targets. Black – TNT with DNT, Blue – TNT with RDX, Red – TNT with p-cresol.*

At this point, we decided to proceed to full characterization of an imprinted (12.6%) 50:50 BTE:DEB hierarchical material. Figure 23 shows the TNT binding isotherm for this material (MM1). We synthesized a similar material (P10) using 50% BTE with 40% DEB and 10% phenyltrimethoxysilane (PTS; Figure 2). The pore size distribution and nitrogen sorption isotherms for this material are presented in Figures 20 and 21. While the material was found to be porous (BET surface area 278 m^2/g; total pore volume 0.226 cm^3/g; pore diameter 43 Å), it was less ordered than the BTE:DEB materials. The ordered macro-structures observed for MM1 were also not present (Figure 24). The advantage of this material was the significant increase in RDX binding capacity. In identical experiments P10 bound more than twice the RDX bound by MM1. The binding capacity of MM1 for TNT was more than twice that of P10. The RDX binding isotherm for P10 is shown in Figure 25.

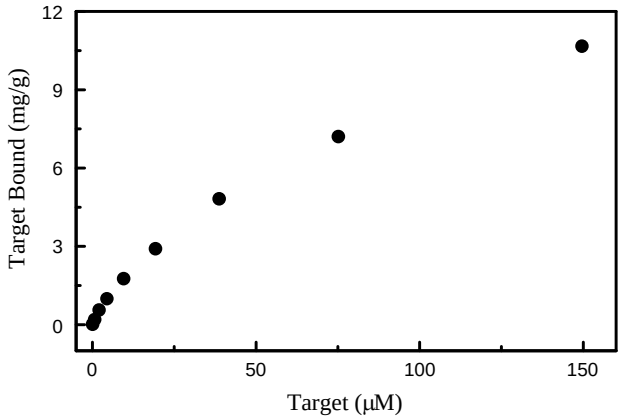

Figure 23. *The TNT binding isotherm for MM1, a 50:50 DEB:BTE hierarchical material imprinted using 12.6% modified Pluronic P123. Here, 15 mg of sorbent was used in a total sample volume of 20 mL.*

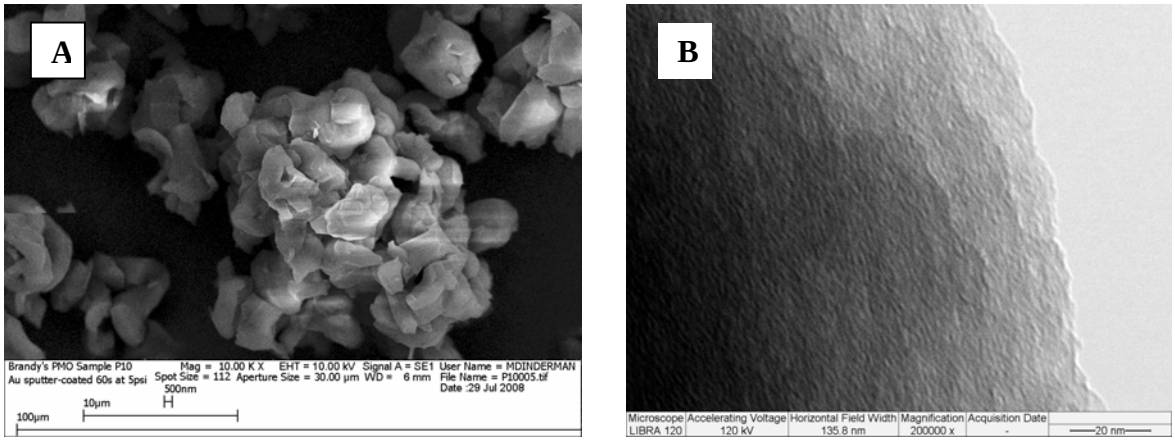

Figure 24. ***A.*** *SEM image of a hierarchical material. This is a 50:40:10 BTE:DEB:PTS material synthesized with no imprint.* ***B.*** *TEM image of the hierarchical material.*

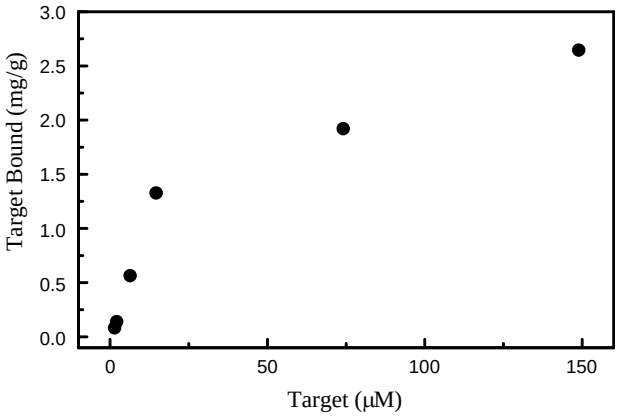

Figure 25. *The RDX binding isotherm for P10, a hierarchical material with terminal phenyl groups incorporated. Here, 15 mg of sorbent was used in a total sample volume of 20 mL.*

The binding isotherms presented here can be used to calculate affinity coefficients similar to those presented in Table 4 for the mesoporous materials. In the case of MM1, the heterogeneity coefficient is not unity; it is 0.39 (*Equation 1*). This indicates that TNT is bound by sites of varying affinity. In the case of P10, holding the heterogeneity coefficient to unity yields a good fit. The affinity coefficient (k) for MM1 is similar to the coefficients obtained for the mesoporous materials while the saturation capacity is significantly higher. The affinity of P10 for RDX is somewhat lower than that of MM1 for TNT.

Table 10. Fit parameters and calculated constants for MM1 and P10 materials.

	slope (m^2)	y-intercept ($m^2/\mu g$)	q_s ($\mu g/m^2$)	k (μg^{-1})
P10 (RDX)	15.3	0.085	11.7	0.006
MM1 (TNT)	0.426	0.005	204.1	0.012

See Table 4 and Equation 1 for explanation of these parameters.

Phase II. Kinetic and Binding Analysis (Batch and Column Studies)

Much of the data necessary for down selecting candidates in Phase I addresses concerns outlined for Phase II of this effort. Extraction efficiencies, affinity coefficients, selectivity, and saturation capacities have been discussed in earlier sections. At this point in the effort, we had

determined that the hierarchical materials offered the best solution to the problems at hand. We had also determined the protocols to be used for synthesis of the materials deemed to be the best candidates. Detailed characterization of the material performance under varying conditions was needed including binding kinetics, impact of pH and temperature, and extraction from complex matrices.

The binding kinetics for MM1 and P10 were found to be slightly slower than that observed for the mesoporous materials (Figures 26 and 27). The reason for this variation was unclear. Studies to evaluate the binding of non-target compounds (p-cresol) to the sites occupied by TNT (or RDX) were conducted (Figures 28 and 29). These types of studies tend to indicate whether or not non-targets will interfere with binding of targets. For both MM1 and P10, p-cresol bound sites not occupied by TNT or RDX (deviation from the line). This indicated that compounds with structures similar to p-cresol were unlikely to compete with the targets for binding sites.

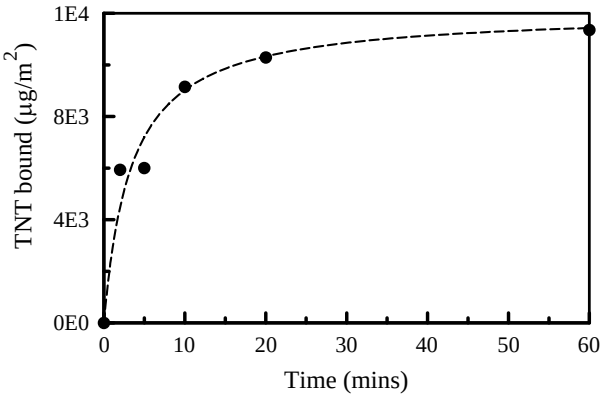

Figure 26. *TNT binding kinetics for MM1. Here, 15 mg of sorbent was used in a total sample volume of 20 mL.*

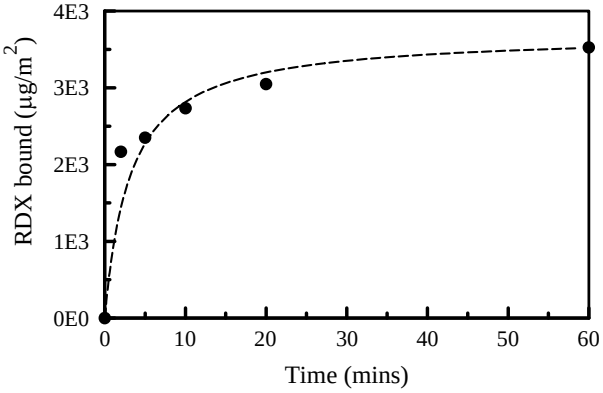

Figure 27. *RDX binding kinetics for P10. Here, 15 mg of sorbent was used in a total sample volume of 20 mL.*

In order to provide a better understanding of how the materials perform, MM1 and P10 were compared with the performance of activated charcoal (Sigma-Aldrich, 0.5 mm particles) in column formats. Each column was prepared with 200 mg of sorbent (MM1, P10, or AC). The data shows the results for 10 successive applications of 3 mL volumes of 10 μM TNT to the columns at a flow rate of 4 mL/min (Figures 30 and 31). Some breakthrough was noted for the activated charcoal columns from the initial application of TNT. The breakthrough threshold for MM1 was not reached during the 10 applications. Based on the calculated saturation capacity (q_s; Table 10), breakthrough would be expected at approximately 15 mg. The performance of MM1 when DNT was selected as the target was nearly identical to the performance observed for TNT. The saturation capacity for the column of P10 was predicted to be approximately 650 μg. This column did not perform as well as expected.

Figure 28. *Linearity study for MM1 binding of TNT in the presence of p-cresol based on Equation 2.*

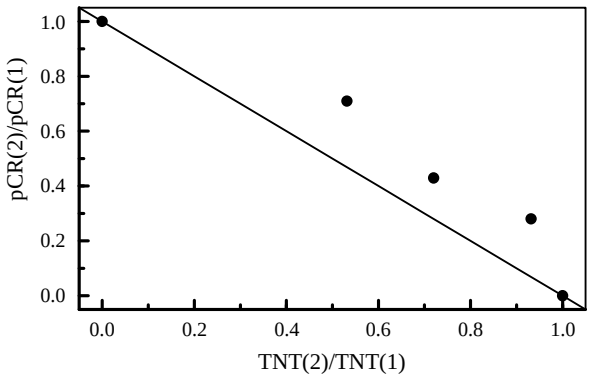

Figure 29. *Linearity study for P10 binding of RDX in the presence of p-cresol based on Equation 2.*

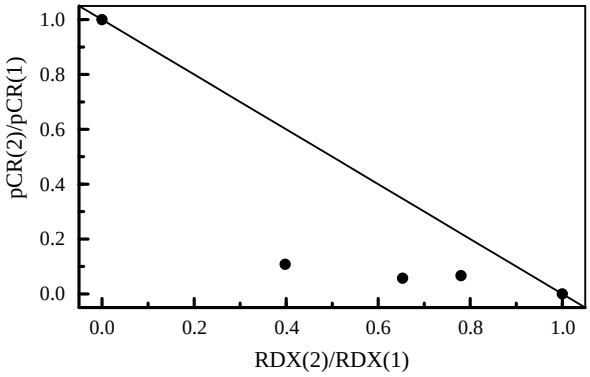

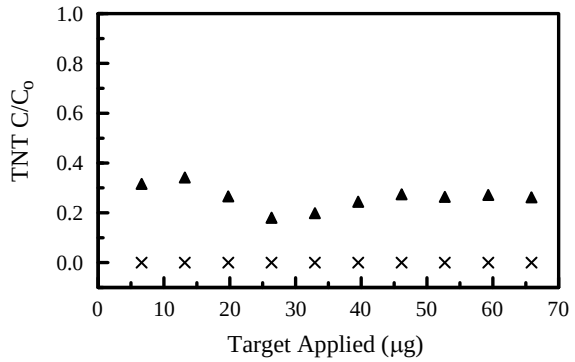

Figure 30. *TNT binding by 200 mg columns of MM1 (x) and activated charcoal (▲).*

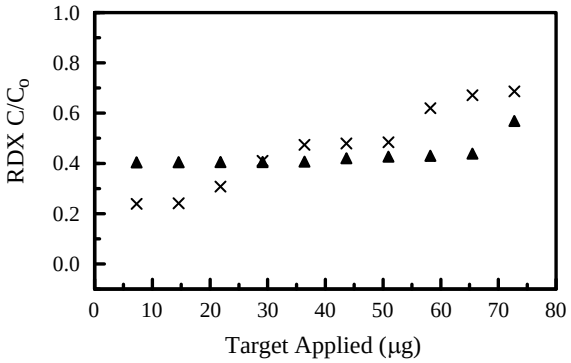

Figure 31. *RDX binding by 200 mg columns of P10 (x) and activated charcoal (▲).*

Binding of targets from more complex matrices was evaluated for both materials. The matrices selected were artificial sea water and pond water collected locally from a park (Alexandria, VA). Binding of TNT by MM1 was not impact significantly by either the pond

water or artificial sea water matrices. Binding of RDX by P10, however, was completely eliminated in both matrices (Figure 32). Because these materials are intended for application in the field for groundwater analysis, P10 was eliminated as a candidate for further evaluation at this point. The impact of temperature and pH on the binding of TNT by MM1 was also evaluated (Figure 33). The sorbent was found to perform similarly over pH values ranging from 4.5 to 9.0. Binding of TNT by MM1 was found to decrease with increasing temperature from 4 to 40°C. This is likely owing to the decreased residence time of the target molecules at higher temperature.

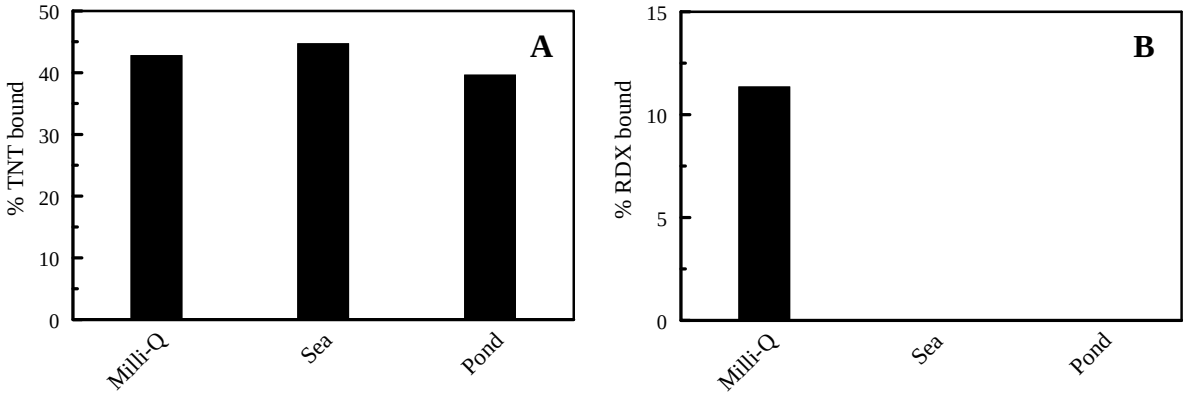

Figure 32. *Binding of targets from complex matrices.* ***A.*** *MM1 binding of TNT.* ***B.*** *P10 binding of RDX. These experiments used 15 mg of sorbent in 20 mL of target solution at 30 μM.*

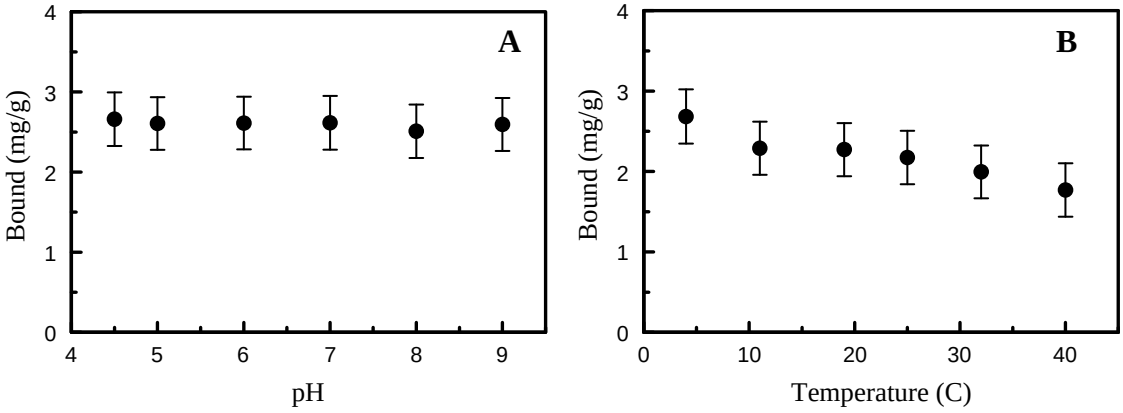

Figure 33. *Binding of TNT from solution by MM1. Experiments were conducted as batch studies using 15 mg of sorbent in 20 mL target solution.* ***A.*** *Varied pH* ***B.*** *Varied temperature*

Phase III: Contaminant Groundwater Testing-Bench/Pilot Demonstration

The focus of Phase III was to evaluate the performance of the materials in real-world samples and to use the materials to concentrate targets prior to analysis by different detection systems. Also of interest was the performance of the materials as compared to commercially available sorbents.

The performance of the sorbent, MM1, was compared to that of two commercially available sorbents. LiChrolut EN is a poly(styrene-divinylbenzene) material available through VWR. PoraPak RDX is a poly(divinylbenzene-vinylpyrrolidone) resin available through Waters. Each of these materials has been described for the concentration of nitroenergetic compounds. Figure 34 shows a side-by-side comparison of these materials to MM1. In each case, 200 mg of sorbent was packed in a polypropylene column. Flow rates for the materials were 4 mL/min. Either 10 or 20 mL of TNT at 100 ppb was applied to the columns. Elution from the columns was accomplished using 1 mL acetonitrile. Concentrations of target in the breakthrough from the columns were below the detection limit in all cases. Acetonitrile was used as the eluent based on the guidance provided with the PoraPak and LiChrolut columns. The data indicate that a high percentage of the target was retained by the PoraPak resin. MM1 was found to yield a higher eluted target concentration than either LiChrolut or PoraPak. Elution of target from MM1 is also possible using methanol rather than acetonitrile with identical results.

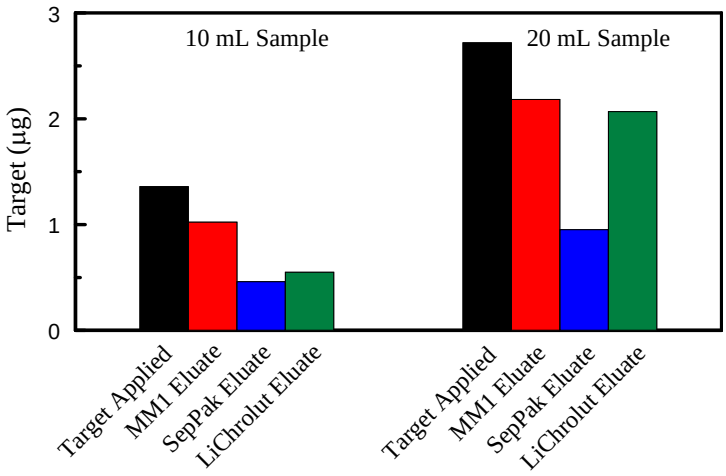

Figure 34. *Side-by-side comparison of MM1 to commercially available pre-concentration resins. Here, 100 ppb TNT in dI-water was used as the target solution.*

During the course of this effort, we were unable to obtain contaminated groundwater samples. We were able to obtain contaminated soil samples as described in the Materials and Methods section. 2 g of each soil sample (Table 11) was placed in 20 mL deionized water and incubated overnight on a rotisserie mixer. The samples were then filtered using 0.2 µm Acrodisc syringe filters. These extracts were applied to a 200 mg MM1 column (10 mL target solution) and eluted using 1 mL methanol. The resulting samples were analyzed by HPLC. Standard curves for a number of targets were generated for comparison and quantification: HMX, RDX, TNB, DNB, tetryl, NB, TNT, 2- and 4-ADNT, 2,4-DNT, and 2-, 3-, 4-NT. Figures 35 and 36 show the results of two such studies. For sample HO-001, the TNT concentration was 6.6 ppm in the soil extract. After pre-concentration, the TNT concentration was found to be 53.7 ppm. The RDX concentration following pre-concentration was double that observed in the soil extract. For HO-022, the concentration of TNT was increased from 0.7 ppm to 6.7 ppm using MM1. The RDX concentration was also increased from 8.5 ppb to 0.5 ppm while the concentration of 2-ADNT was increased to 62 ppb from an undetectable level. Figure 37 presents a summary of the results obtained for all of the soil samples. Full results including concentrations are available in Appendix A. MM1 was determined to provide pre-concentration of a number of the targets present in these 12 samples.

Table 11. *Soil samples.*

Sample Name	Site Type	
HO-001	Old 2,000-lb bomb crater	
HO-004	Old 2,000-lb bomb crater	
HO-006	Old 500-lb bomb crater	
HO-018	Low order bomb crater	Hot Grid
HO-019	Low order bomb crater	Hot Grid
HO-020	Low order bomb crater	Hot Grid
HO-022	2,000-lb bomb crater	Hot Grid
HO-023	2,000-lb bomb crater	Hot Grid
HO-024	2,000-lb bomb crater	Hot Grid
HO-025	No visible low-order debris	Cold Grid
HO-026	No visible low-order debris	Cold Grid
HO-027	No visible low-order debris	Cold Grid

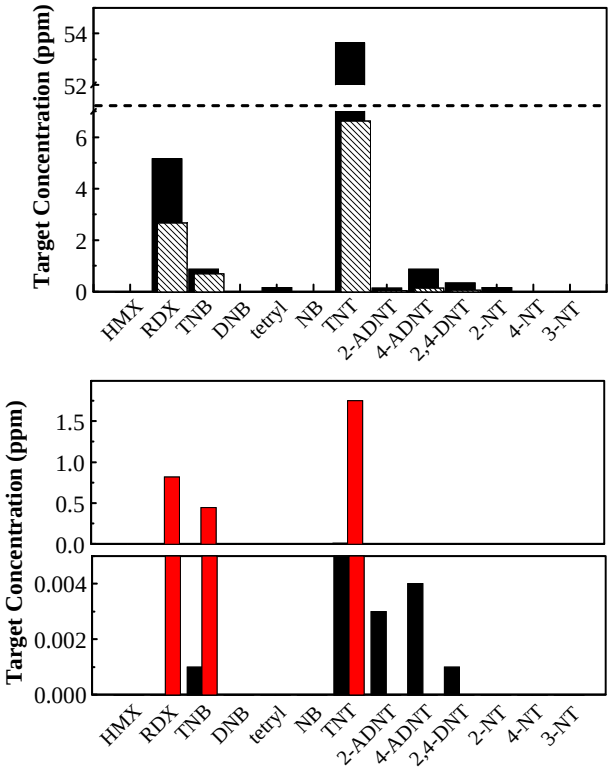

Figure 35. *Concentration of soil sample extract (HO-001) using MM1.* ***A.*** *Shown here are the concentration of the targets in the soil extract before (hashed) and after preconcentration (solid).* ***B.*** *This panel presents the concentrations of the targets reported by USERDC (black) and the concentrations detected in the column breakthrough (red).*

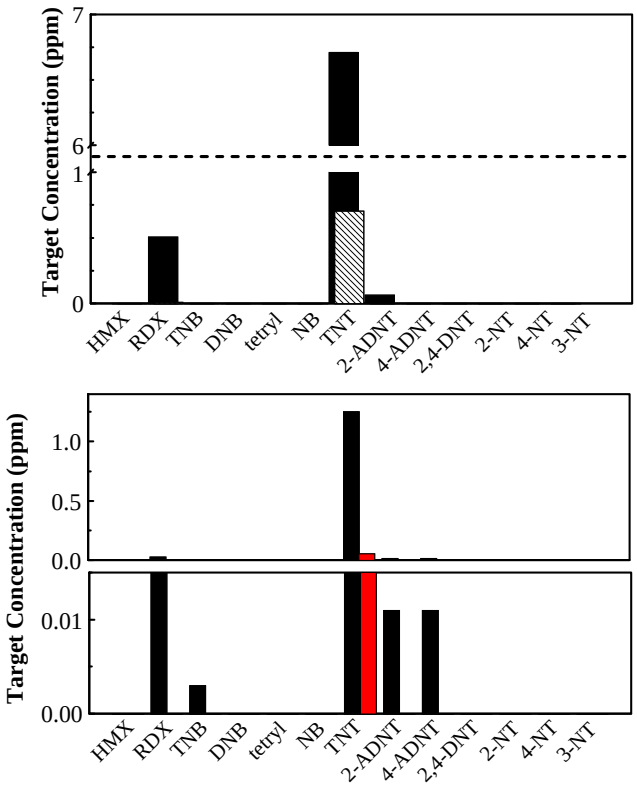

Figure 36. *Concentration of soil sample extract (HO-022) using MM1.* ***A.*** *Shown here are the concentration of the targets in the soil extract before (hashed) and after preconcentration (solid).* ***B.*** *This panel presents the concentrations of the targets reported by USERDC (black) and the concentrations detected in the column breakthrough (red).*

Concluding Summary

In our early studies, the binding capacity of the BTE-DEB co-condensates was found to be strongly dependent upon the DEB content of the materials, however, as the DEB content of the materials was increased binding of non-target compounds also increased. M-70:30 offered a compromise in that it displayed a marked enhancement in TNT binding over that observed with the BTE only material while binding of compounds such as pNP and pCr was not strongly increased. In addition, imprinting of M-70:30 (M-70:30 Imp; 12.5% DNB-Brij) produced TNT binding which was apparently independent of the presence of pNP and pCr. While the TNT binding capacity of M-70:30 could be further enhanced through the exclusive use of DNB-Brij as the surfactant, M-70:30 Imp 100 absorption of TNT was highly non-specific and was subject to reduction when pNP and pCr were present. In addition, the reduced degree of order and pore size homogeneity in this material, as noted in Figures 13 to 15, resulted in the slowest adsorption kinetics observed. Equilibrium adsorption was reached after 30 mins for M-70:30 Imp 100 while in more ordered materials, such as M-70:30 and M-70:30 Imp, equilibrium adsorption was attained in less than 3 mins. In order to obtain the selective materials desired, a sacrifice in total capacity was necessary. M-70:30 Imp 50 did not offer any advantages over M-70:30 Imp, while it consumed much more of the DNB-Brij template molecule. M-70:30 Imp appeared to offer the best combination of binding capacity and selectivity for TNT.

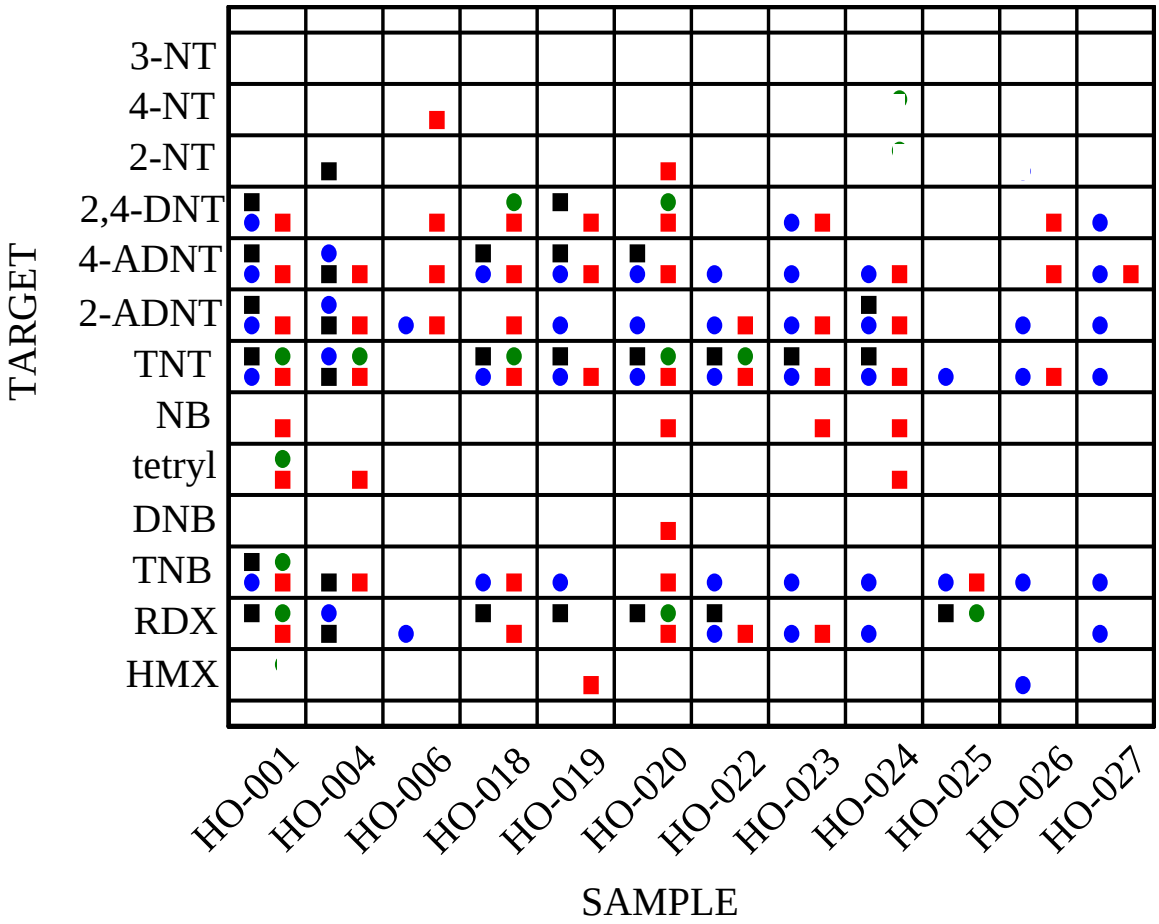

Figure 37. *Summary of results from soil samples. A symbol in the box indicates detection in the relevant sample. black – soil extract; red – eluate; green – breakthrough; blue - USERDC*

The imprinting technique applied to the materials used in this study employed a new type of template molecule. Previously, the target analog employed for molecular imprinting was a ten carbon chain terminated with a di- or trinitrobenzene group.[32; 33] Because it had low water solubility, it is likely that the majority of this molecule was contained within the hydrophobic cores of the Brij®76 micelles. In this case, there was little contact with the pore walls during condensation. This limited contact was reflected by the only marginal success obtained using this molecule for imprinting. The modified version of Brij®76 used here was definitively successful. Inclusion of this template into the micelles was more favorable than for the previous template and the DNB groups were exposed to the pore walls. We have also been able to show that this technique is adaptable to the generation of templates against other targets of interest. We have imprinted a porous material using Pluronic P123 modified using diethyl chlorophosphate, an analog for paraoxon. The material shows selectivity for paraoxon and excludes p-nitrophenol (Figure 38).(unpublished results; [19])

Paraoxon **Diethyl chlorophosphate** **p-Nitrophenol**

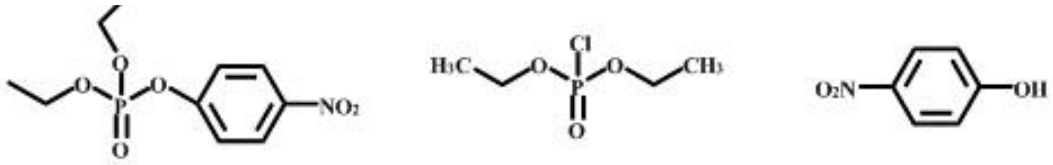

Figure 38. *Diethyl chlorophosphate is used as an imprint template in a material designed for selective binding of paraoxon. This material binds very little p-nitrophenol and the two compounds do not compete for binding sites.*

In order to address the back pressure issues typically encountered when employing mesoporous materials in column formats, we altered the synthesis of the materials to include a larger surfactant combined with a swelling agent. These changes result in materials with order on two length scales. The mesopores are slightly larger than those of the earlier materials, and they are along the pore walls of macropores of about 1 μm. This technique sacrifices some of the surface area of the mesoporous materials, but it improves interconnectivity. In fact, the saturation capacity of the hierarchical materials is greater than that of the earlier mesoporous materials while the affinity coefficient is only slightly reduced. In order to optimize the synthesis of this new type of material, variations in precursor ratios, template to surfactant ratios, and acid and swelling agent concentrations were evaluated. It was determined that a 50:50 DEB:BTE material (7.84 mmol total precursor) imprinted with 12.6% modified Pluronic P123 using 0.55 g mesitylene and 7.5 g 0.1 M nitric acid provided the optimal material for these applications.

An additional hierarchical material was synthesized in which phenyltrimethoxysilane was used as 10% of the total precursor. This modification to the material was found to enhance RDX binding. Both MM1 (50:50 DEB:BTE material) and P10 (50:40:10 DEB:BTE:PTS) were evaluated for target extraction. While P10 was found to semi-selectively remove RDX, it was also found that target binding was abrogated by complex matrices such as artificial sea water and pond water. The material was deemed unsuitable for application to real-world samples. Materials with other bridging groups (such as 4-4'-bis(triethoxysilyl)biphenyl; Figure 2) were found to have lower affinities and capacities for RDX and TNT than MM1. On the basis of these studies, MM1 was selected as the candidate for further evaluation.

MM1 was compared to two commercially available resins described for the concentration of nitroenergetics. The material provided more concentrated target in the eluate than either of the commercial polymer resins. The material was used for pre-concentration of targets from soil samples collected by the US Army Corps of Engineers, Engineer Research and Development Center from sites at Holloman Air Force Base, Alamogordo, NM. MM1 concentrated a number of targets from these samples including: TNT, DNT, 2- and 4-ADNT, TNB, and RDX. Side-by-side comparison of MM1 to the commercial resins using spiked groundwater samples was ongoing at the time of this report. A single column of MM1 was used for concentration of more

than 75 samples including deionized water preparations, soil extract, and groundwater samples with no loss of function.

Interest in these types of materials for the concentration of compounds such as trichloroethylene and tetrachloroethylene has been expressed by Dr. M. Gribb (Boise State University) and Dr. H. Hill (Washington State University). We are currently working to establish a Materials Transfer Agreement (MTA) with Seacoast Science Inc (Carlsbad, CA). This company is interested in evaluating the potential of these materials for use with gas chromatography systems. There is an additional group within NRL (A. Kusterbeck) working with SubChem (Narragansett, RI) to design an electrochemical sensor for use with the REMUS (Remote Environmental Monitoring Units) UUA. The group is planning to use the materials developed during the course of this program to pre-concentrate nitroenergetic targets from sea water. Their current work is being funded through ONR. SubChem has also expressed a willingness to work directly with our group to design remote sensing systems. SubChem has significant engineering experience with these types of projects. Shown below are images of several SubChem projects: the ChemFin Analyzer; the Gateway buoy; a fixed, bottom-mount sensor assembly; and the REMUS (Figure 39). In addition to these types of active monitoring applications, the material developed during the course of this program has the potential for deployment for short- and long-term passive monitoring similar to the polyethylene passive sampling materials.

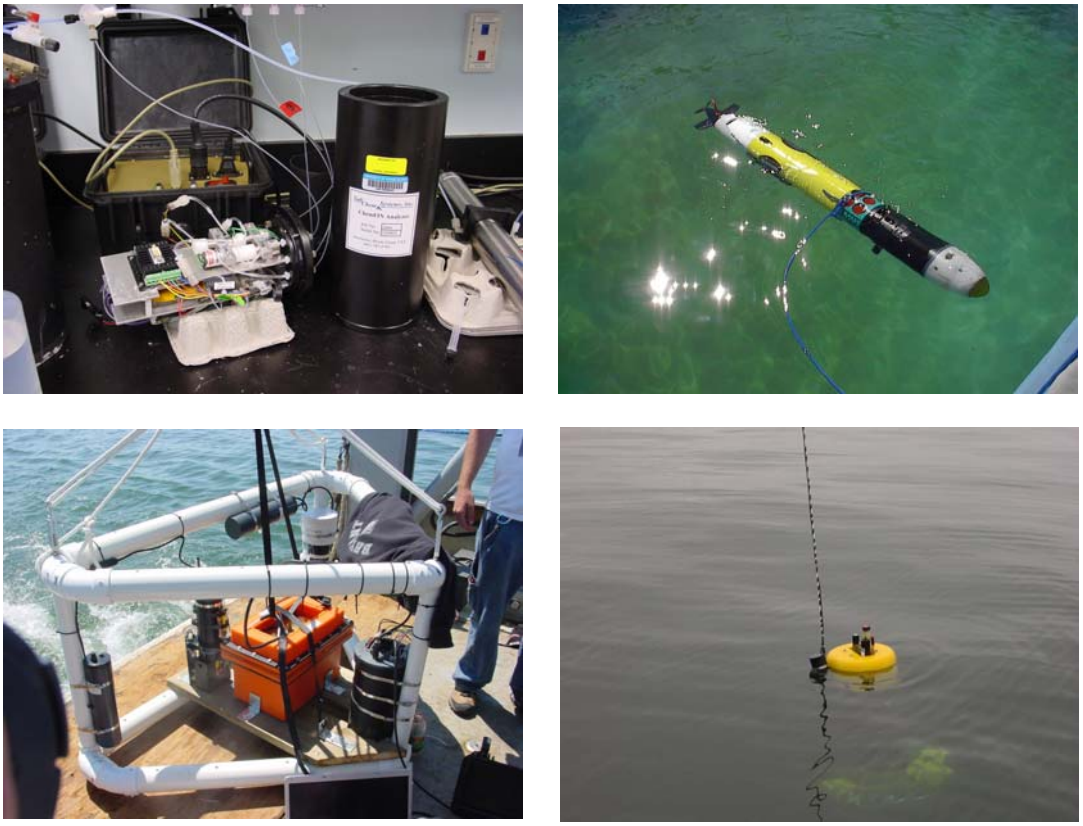

Figure 39. *SubChem projects:* ***A.*** *ChemFin Analyzer;* ***B.*** *REMUS;* ***C.*** *Fixed, bottom-mount sensor assembly;* ***D.*** *Gateway buoy.*

References

[1] R.F. Spalding, and J.W. Fulton, Groundwater munition residues and nitrate near Grand Island, Nebraska, U.S.A. Journal of Contaminant Hydrology 2 (1998) 139-153.

[2] J.C. Spain, Biodegradation of Nitroaromatic Compounds. Annual Review of Microbiology 49 (1995) 523-555.

[3] J.C. Spain, J.B. Hughes, and H.-J. Knackmuss, (Eds.), Nitroaromatic Compounds and Explosivies, CRC Press, Boca Raton, 2000.

[4] K.T. Valsaraj, K.M. Qaisi, W.D. Constant, L.J. Thibodeaux, and K.S. Ro, Diffusive transport of 2,4,6-trinitrotoluene (TNT) from contaminated soil to overlying water. Journal of Hazardous Materials 59 (1998) 1-12.

[5] J. Yinon, (Ed.), Toxicity and Metabolism of Explosives, CRC Press, Boca Raton, 1990.

[6] T.F. Jenkins, P.H. Miyares, K.F. Myers, E.F. McCormick, and A.B. Strong, Comparison of solid-phase extraction with salting-out solvent-extraction for preconcentration of nitroaromatic and nitramine explosives from water. Analytica Chimica Acta 289 (1994) 69-78.

[7] D.C. Leggett, T.F. Jenkins, and P.H. Miyares, Salting-out solvent-extraction for preconcentration of neutral polar organic solutes from water. Analytical Chemistry 62 (1990) 1355-1356.

[8] F. Monteil-Rivera, C. Beaulieu, and J. Hawari, Use of solid-phase microextraction/gas chromatography-electron capture detection for the determination of energetic chemicals, in marine samples. Journal of Chromatography A 1066 (2005) 177-187.

[9] C. Crescenzi, J. Albinana, H. Carlsson, E. Holmgren, and R. Batlle, On-line strategies for determining trace levels of nitroaromatic explosives and related compounds in water. Journal of Chromatography a 1153 (2007) 186-193.

[10] M. Smith, G.E. Collins, and J. Wang, Microscale solid-phase extraction system for explosives. Journal of Chromatography a 991 (2003) 159-167.

[11] T. Asefa, M.J. MacLachlan, N. Coombs, and G.A. Ozin, Periodic mesoporous organosilicas with organic groups inside the channel walls. Nature 402 (1999) 867-871.

[12] S. Inagaki, Guan, S., Fukushima, Y., Ohsuna, T., Terasaki, O. , Novel mesoporous materials with a uniform distribution of organic groups and inorganic oxide in their frameworks. J. Am. Chem. Soc. 121 (1999) 9611-14.

[13] B.J. Melde, B.T. Holland, C.F. Blanford, and A. Stein, Mesoporous Sieves with Unified Hybrid Inorganic/Organic Frameworks. Chem. Mater. 11 (1999) 3302-3308.

[14] M.C. Burleigh, M.A. Markowitz, M.S. Spector, and B.P. Gaber, Porous organosilicas: An acid-catalyzed approach. Langmuir 17 (2001) 7923-7928.

[15] Y. Goto, and S. Inagaki, Synthesis of large-pore phenylene-bridged mesoporous organosilica using triblock copolymer surfactant. Chemical Communications (2002) 2410-2411.

[16] C.T. Kresge, M.E. Leonowicz, W.J. Roth, J.C. Vartuli, and J.S. Beck, Ordered mesoporous molecular sieves synthesized by a liquid-crystal template mechanism. Nature 359 (1992) 710-712.

[17] R.J.P. Corriu, and D. Leclercq, Recent developments of molecular chemistry for sol-gel processes. Angewandte Chemie-International Edition in English 35 (1996) 1420-1436.

[18] Q.S. Huo, D.I. Margolese, and G.D. Stucky, Surfactant control of phases in the synthesis of mesoporous silica-based materials. Chemistry of Materials 8 (1996) 1147-1160.
[19] B.J. White, B.J. Melde, and P.T. Charles, Ongoing work funded through DTRA - Protection and Hazard Mitigation. (2008).
[20] M.C. Burleigh, M.A. Markowitz, M.S. Spector, and B.P. Gaber, Porous polysilsesquioxanes for the adsorption of phenols. Environmental Science & Technology 36 (2002) 2515-2518.
[21] U. Lewin, J. Efer, and W. Engewald, High-performance liquid chromatographic analysis with electrochemical detection for residues of explosives in water samples around a former ammunition plant, 19th International Symposium on Column Liquid Chromatography, Innsbruck, Austria, 1995, pp. 161-167.
[22] J. Wang, R.K. Bhada, J.M. Lu, and D. MacDonald, Remote electrochemical sensor for monitoring TNT in natural waters. Analytica Chimica Acta 361 (1998) 85-91.
[23] C. Sun, M. Baird, H.A. Anderson, and D.L. Brydon, Separation and determination of oligomers and homologues of aliphatic alcohol ethoxylates in textile lubricants and lubricant emulsion by high-performance liquid chromatography. Journal of Chromatography A 771 (1997) 145-154.
[24] M.C. Burleigh, M.A. Markowitz, M.S. Spector, and B.P. Gaber, Porous polysilsesquioxanes for the adsorption of phenols. Environ Sci Technol 36 (2002) 2515-18.
[25] M.C. Burleigh, S. Jayasundera, C.W. Thomas, M.S. Spector, M.A. Markowitz, and B.P. Gaber, A versatile synthetic approach to periodic mesoporous organosilicas. Colloid and Polymer Science 282 (2004) 728-733.
[26] S.A. Bagshaw, and T.J. Pinnavaia, Mesoporous alumina molecular sieves. Angewandte Chemie-International Edition in English 35 (1996) 1102-1105.
[27] S.A. Bagshaw, E. Prouzet, and T.J. Pinnavaia, TEMPLATING OF MESOPOROUS MOLECULAR-SIEVES BY NONIONIC POLYETHYLENE OXIDE SURFACTANTS. Science 269 (1995) 1242-1244.
[28] H.J. Kim, and G. Guiochon, Comparison of the thermodynamic properties of particulate and monolithic columns of molecularly imprinted copolymers. Analytical Chemistry 77 (2005) 93-102.
[29] R.J. Umpleby, S.C. Baxter, M. Bode, J.K. Berch, R.N. Shah, and K.D. Shimizu, Application of the Freundlich adsorption isotherm in the characterization of molecularly imprinted polymers. Analytica Chimica Acta 435 (2001) 35-42.
[30] C. Ockrent, Selective absorption by activated charcoal from solutions containing two organic acids. Journal of the Chemical Society (1932) 613-630.
[31] W.J. Weber, Competitive interactions in adsorption from dilute aqueous bi-solute solutions. Journal of Applied Chemistry of the Ussr 14 (1964) 565-572.
[32] B. Johnson-White, M. Zeinali, A.P. Malanoski, and M.A. Dinderman, Sunlight-catalyzed Conversion of Cyclic Organics with Novel Mesoporous Organosilicas. Catal. Commun. 8 (2007) 1052-1056.
[33] B. Johnson-White, M. Zeinali, K.M. Shaffer, J. C. H. Patterson, P.T. Charles, and M.A. Markowitz, Detection of organics using porphyrin embedded nanoporous organosilicas. Biosens. Bioelect. 22 (2007) 1154-1162.

Appendix A: Supporting Information

Soil Sample Results

			HMX (ppm)				RDX (ppm)				trinitrobenzene (ppm)			
Sample	Site Type		USERDC	Extract	Eluate	Residual	USERDC	Extract	Eluate	Residual	USERDC	Extract	Eluate	Residual
HO-001	Old 2,000-lb bomb crater		0	0	0	0	0	2.678	5.155	0.824	0.001	0.694	0.861	0.445
HO-004	Old 2,000-lb bomb crater		0	0	0	0	0.001	0.120	0	0	0.003	0	0.308	0
HO-006	Old 500-lb bomb crater		0	0	0	0	0.001	0	0	0	0	0	0	0
HO-018	Low order bomb crater	Hot Grid	0	0	0	0	0	0.084	0.100	0	0.001	0	0.078	0
HO-019	Low order bomb crater	Hot Grid	0	0	0.448	0	0	0.197	0	0	0.001	0	0	0
HO-020	Low order bomb crater	Hot Grid	0	0	0	0	0	0.223	0.035	0.235	0	0	0.263	0
HO-022	2,000-lb bomb crater	Hot Grid	0	0	0	0	0.025	0.008	0.504	0	0.003	0	0	0
HO-023	2,000-lb bomb crater	Hot Grid	0	0	0	0	0.004	0	0.336	0	0.003	0	0	0
HO-024	2,000-lb bomb crater	Hot Grid	0	0	0	0	0.001	0	0	0	0.001	0	0	0
HO-025	No visible low-order debris	Cold Grid	0	0	0	0	0	0.213	0	0.101	0.008	0	0.031	0
HO-026	No visible low-order debris	Cold Grid	0.001	0	0	0	0	0	0	0	0.003	0	0	0
HO-027	No visible low-order debris	Cold Grid	0	0	0	0	0.002	0	0	0	0.002	0	0	0

			2,4-dinitrotoluene (ppm)				tetryl (ppm)				nitrobenzene (ppm)			
Sample	Site Type		USERDC	Extract	Eluate	Residual	USERDC	Extract	Eluate	Residual	USERDC	Extract	Eluate	Residual
HO-001	Old 2,000-lb bomb crater		0	0	0	0	N/A	0	0.150	0	N/A	0	0	0
HO-004	Old 2,000-lb bomb crater		0	0	0	0	N/A	0	0.050	0	N/A	0	0	0
HO-006	Old 500-lb bomb crater		0	0	0	0	N/A	0	0	0	N/A	0	0	0
HO-018	Low order bomb crater	Hot Grid	0	0	0	0	N/A	0	0	0	N/A	0	0	0
HO-019	Low order bomb crater	Hot Grid	0	0	0	0	N/A	0	0	0	N/A	0	0	0
HO-020	Low order bomb crater	Hot Grid	0	0	0.027	0	N/A	0	0	0	N/A	0	0.066	0
HO-022	2,000-lb bomb crater	Hot Grid	0	0	0	0	N/A	0	0	0	N/A	0	0	0
HO-023	2,000-lb bomb crater	Hot Grid	0	0	0	0	N/A	0	0	0	N/A	0	0.032	0
HO-024	2,000-lb bomb crater	Hot Grid	0	0	0	0	N/A	0	0.081	0	N/A	0	0.032	0
HO-025	No visible low-order debris	Cold Grid	0	0	0	0	N/A	0	0	0	N/A	0	0	0
HO-026	No visible low-order debris	Cold Grid	0	0	0	0	N/A	0	0	0	N/A	0	0	0
HO-027	No visible low-order debris	Cold Grid	0	0	0	0	N/A	0	0	0	N/A	0	0	0

			2,4,6-trinitrotoluene (ppm)				4-amino-2,6-dinitrotoluene (ppm)				2-amino-4,6-dinitrotoluene (ppm)			
Sample	Site Type		USERDC	Extract	Eluate	Residual	USERDC	Extract	Eluate	Residual	USERDC	Extract	Eluate	Residual
HO-001	Old 2,000-lb bomb crater		0.014	6.615	53.658	1.754	0.003	0.049	0.136	0	0.004	0.144	0.864	0
HO-004	Old 2,000-lb bomb crater		0.005	0.298	2.959	0.036	0.002	0.040	0.067	0	0.002	0.018	0.391	0
HO-006	Old 500-lb bomb crater		0	0	0	0	0.001	0	0.004	0	0	0	0.072	0
HO-018	Low order bomb crater	Hot Grid	0.015	0.680	6.839	0.065	0	0	0.164	0	0.004	0.092	1.041	0
HO-019	Low order bomb crater	Hot Grid	0.054	0.693	5.217	0	0.004	0	0	0	0.001	0.128	0.987	0
HO-020	Low order bomb crater	Hot Grid	0.202	1.039	11.868	0.008	0.005	0	0	0	0.004	0.099	1.521	0
HO-022	2,000-lb bomb crater	Hot Grid	1.250	0.704	6.710	0.054	0.011	0	0.062	0	0.011	0	0	0
HO-023	2,000-lb bomb crater	Hot Grid	0.260	0.096	1.697	0	0.012	0	0.095	0	0.009	0	0	0
HO-024	2,000-lb bomb crater	Hot Grid	0.270	0.070	1.621	0	0.012	0.008	0.061	0	0.011	0	0.268	0
HO-025	No visible low-order debris	Cold Grid	0.058	0	0	0	0	0	0	0	0	0	0	0
HO-026	No visible low-order debris	Cold Grid	0.019	0	0.049	0	0.006	0	0	0	0	0	0.032	0
HO-027	No visible low-order debris	Cold Grid	0.008	0	0	0	0.011	0	0	0	0.003	0	0.016	0

			2,4-dinitrotoluene (ppm)				2,4-dinitroaniline (ppm)				2-nitrotoluene (ppm)			
Sample	Site Type		USERDC	Extract	Eluate	Residual	USERDC	Extract	Eluate	Residual	USERDC	Extract	Eluate	Residual
HO-001	Old 2,000-lb bomb crater		0.001	0.065	0.343	0	0	N/A	N/A	N/A	N/A	0	0.159	0
HO-004	Old 2,000-lb bomb crater		0	0	0	0	0.001	N/A	N/A	N/A	N/A	0	0	0
HO-006	Old 500-lb bomb crater		0	0	0.018	0	0	N/A	N/A	N/A	N/A	0	0	0
HO-018	Low order bomb crater	Hot Grid	0	0	0.071	0.004	0	N/A	N/A	N/A	N/A	0	0	0
HO-019	Low order bomb crater	Hot Grid	0	0.018	0.040	0	0	N/A	N/A	N/A	N/A	0	0	0
HO-020	Low order bomb crater	Hot Grid	0	0	0.071	0.004	0	N/A	N/A	N/A	N/A	0	0.097	0
HO-022	2,000-lb bomb crater	Hot Grid	0	0	0	0	0	N/A	N/A	N/A	N/A	0	0	0
HO-023	2,000-lb bomb crater	Hot Grid	0.008	0	0.034	0	0	N/A	N/A	N/A	N/A	0	0	0
HO-024	2,000-lb bomb crater	Hot Grid	0	0	0	0	0	N/A	N/A	N/A	N/A	0	0	0
HO-025	No visible low-order debris	Cold Grid	0	0	0	0	0	N/A	N/A	N/A	N/A	0	0	0
HO-026	No visible low-order debris	Cold Grid	0	0	0.001	0	0.001	N/A	N/A	N/A	N/A	0	0	0
HO-027	No visible low-order debris	Cold Grid	0.001	0	0	0	0	N/A	N/A	N/A	N/A	0	0	0

			4-nitrotoluene (ppm)				3-nitrotoluene (ppm)			
Sample	Site Type		USERDC	Extract	Eluate	Residual	USERDC	Extract	Eluate	Residual
HO-001	Old 2,000-lb bomb crater		N/A	0	0	0	N/A	0	0	0
HO-004	Old 2,000-lb bomb crater		N/A	0	0	0	N/A	0	0	0
HO-006	Old 500-lb bomb crater		N/A	0	0.048	0	N/A	0	0	0
HO-018	Low order bomb crater	Hot Grid	N/A	0	0	0	N/A	0	0	0
HO-019	Low order bomb crater	Hot Grid	N/A	0	0	0	N/A	0	0	0
HO-020	Low order bomb crater	Hot Grid	N/A	0	0	0	N/A	0	0	0
HO-022	2,000-lb bomb crater	Hot Grid	N/A	0	0	0	N/A	0	0	0
HO-023	2,000-lb bomb crater	Hot Grid	N/A	0	0	0	N/A	0	0	0
HO-024	2,000-lb bomb crater	Hot Grid	N/A	0	0	0	N/A	0	0	0
HO-025	No visible low-order debris	Cold Grid	N/A	0	0	0	N/A	0	0	0
HO-026	No visible low-order debris	Cold Grid	N/A	0	0	0	N/A	0	0	0
HO-027	No visible low-order debris	Cold Grid	N/A	0	0	0	N/A	0	0	0

USERDC – results obtained by USERDC using EPA Method 8330B
Extract, Eluate, Residual – results of HPLC analysis using modified Method 8330 as described on page 13
Extract – concentration of targets in soil samples processed as described on page 37
Eluate – concentration of targets in sample resulting from elution of targets from sorbent using methanol
Residual – concentration of targets in column effluent (water)
"0" indicates levels below the detection threshold
N/A indicates targets not evaluated

Cost Analysis

The following data provides cost information for small scale production of MM1 as described in the Results and Accomplishments section at the time of this report. Large scales production would be expected to significantly reduce costs.

Chemicals	**Unit Size**	**Cost**	**Supplier**
1,2-bis(trimethoxysilyl)ethane	25 mL	$85.10	Sigma-Aldrich
bis(trimethoxysilylethyl)benzene	50 g	$132.00	Gelest, Inc.
Mesitylene	500 mL	$59.30	Sigma-Aldrich
Pluronic P123	1 L	$62.40	Sigma-Aldrich
nitric acid, 70%	500 mL	$39.20	Sigma-Aldrich
dichloromethane, ≥98%	1 L	$44.70	Sigma-Aldrich
Ethanol	1 pint	$2.00	Warner-Graham Company
3,5-dinitrobenzoyl chloride	25 g	$30.10	Sigma-Aldrich
magnesium turnings	250 g	$134.50	Sigma-Aldrich
sodium bicarbonate	500 g	$32.70	Sigma-Aldrich

Synthesis of Pluronic P123 imprint template; esterification of Pluronic P123 with 3,5-dinitrobenzoyl chloride.

Chemicals	**Amount**	**Cost**
Pluronic P123	8 g	$0.50
3,5-dinitrobenzoyl chloride	1.27 g	$1.53
dicloromethane	60 mL	$2.68
sodium bicarbonate	1.2 g	$0.08
magnesium turnings	0.2 g	$0.11
	Total	$4.90

Synthesis of the imprinted hierarchical BTE:DEB sorbent; batch size is approximately 2 g.

Chemicals	**Amount**	**Cost**
1,2-bis(trimethoxysilyl)ethane	0.988 mL	$3.36
bis(trimethoxysilylethyl)benzene	1.468 g	$3.88
mesitylene	0.64 mL	$0.08
Pluronic P123	1.66 mL	$0.10
imprint surfactant	0.24 g	$0.15
nitric acid	7.5 g 0.1 M	<$0.01
ethanol	1250 mL	$5.29
	Total	$12.86

Appendix B: List of Technical Publications

Peer-reviewed journal articles

"Mesoporous Silicate Materials in Sensing" B.J. Melde, B.J. Johnson, P.T. Charles. *Sensors*, 8 (8), 5202-28 (2008).

"Imprinted Nanoporous Organosilicas for Selective Adsorption of Nitroenergetic Targets" B.J. Johnson, B.J. Melde, P.T. Charles, D.C. Cardona, M.A. Dinderman, A.P. Malanoski, S. Qadri. *Langmuir*, 224, 9024-9 (2008).

"Macroporous Silica for Concentration of Nitroenergetic Targets" B.J. Johnson, B.J. Melde, P.T. Charles, M.A. Dinderman, A.P. Malanoski, *Manuscript in Preparation*, (2009).

"Macroporous Monoliths of Multifunctional Periodic Mesoporous Organosilicas" B.J. Melde, B.J. Johnson, M.A. Dinderman, S. Qadri., *Manuscript in Preparation*, (2009).

Published technical abstracts

"Imprinted Nanoporous Organosilicas for Selective Adsorption of Nitroenergetic Targets" B.J. White, P.T. Charles, B.J. Melde *SERDP & ESTCP's Partners in Environmental Technology Technical Symposium & Workshop*; Washington, DC; December 2-4, 2008.